Aquaculture 610 (2026) 742851

Contents lists available at ScienceDirect

Aquaculture

journal homepage: www.elsevier.com/locate/aquaculture

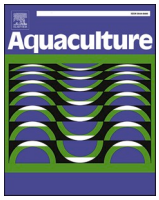

Health, microbiota, and water quality analysis: A case study in a commercial recirculating aquaculture system for yellowtail kingfish (*Seriola lalandi*).

Katerina Loufi [a,1], Julia Hassa [b,c,1], Eric Hernández [d], Marit Stormoen [e], Deni Ribičić [g], Stamatios Kapasakis [h], Tobias Busche [b,c], Jörn Kalinowski [b], Pavlos Makridis [a], Roman Netzer [e], Elia Ciani [e,f,*]

[a] *Department of Biology, University of Patras, Rio Achaias, Greece*
[b] *Center for Biotechnology (CeBiTec), Bielefeld University, Germany*
[c] *Medical School East Westphalia-Lippe, Bielefeld University, Germany*
[d] *Blue Revolution Center, InfiniteSea GmbH, Völklingen, Germany*
[e] *Department of Production Animal Clinical Sciences, Norwegian University of Life Sciences, Ås, Norway*
[f] *Aquaculture and Hydrobiology Unit, Edmund Mach Foundation, San Michele all'Adige, Trento, Italy*
[g] *Department of Aquaculture, SINTEF Ocean AS, Trondheim, Norway*
[h] *Department of Biotechnology and Food Science, Norwegian University of Science and Technology, Trondheim, Norway*

ARTICLE INFO

Keywords:
RAS
Microbiota
Histology
Fish health
Sustainable aquaculture

ABSTRACT

This study describes the temporal and spatial dynamics of microbiota composition, water quality parameters and fish health status in a commercial Recirculating Aquaculture System (RAS) for yellowtail kingfish (*Seriola lalandi*) spanning from April to November 2021. Water quality was effectively controlled, with key parameters such as CO_2, pH, temperature, nitrogen compounds and hydrogen sulfide (H_2S) consistently maintained within safety thresholds reported in the literature. Microbiota composition was analyzed in various fish tissues and RAS components using 16S rRNA gene amplicon sequencing. The predominant genera in RAS samples (tank water, tank wall biofilm, biofilter biofilm, and denitrification unit) included *Erythrobacter*, *Glaciecola*, and *Nitrospira*. In contrast, fish tissue samples (gills, intestine, and skin) were mainly colonized by *Aliivibrio*, *Pseudomonas*, and an uncultured genus from the *Mycoplasmataceae* family. Cluster analysis revealed similarities in bacterial composition between tank water and external fish tissues (skin and gills), with variations over time corresponding to changes in water parameters. Digital PCR assays were developed to target specific fish pathogens such as *Vibrio harveyi*, *Vibrio anguillarum*, and *Photobacterium damselae piscicida*, revealing low or undetectable pathogen levels throughout most of the monitoring period. In tank water, these species showed the highest concentration in August and September. A Multiparametric Semi-quantitative Scoring System (MSSS) was developed for histological examination of gills, intestine, liver, spleen, and kidney. Increased inflammation coincided with higher pathogen presence in the water. However, no clinical signs of vibriosis or pasteurellosis were detected, indicating overall good fish health and a robust immune system. This integrated approach - combining innovative pathogen-specific digital PCR assays, MSSS histological scoring and microbiota profiling offers a valuable framework for monitoring fish health and optimizing production quality in kingfish farming within RAS environments.

1. Introduction

The yellowtail kingfish (*Seriola lalandi*) is a carnivorous, pelagic marine fish that inhabits subtropical and temperate waters in the Pacific and Indian Oceans (Fowler et al., 2003). Known for its high growth rates and widespread market acceptance, this species is favored for

* Corresponding author.
E-mail address: elia.ciani@fmach.it (E. Ciani).
[1] The authors contributed equally to the study.

https://doi.org/10.1016/j.aquaculture.2025.742851
Received 29 August 2024; Received in revised form 11 June 2025; Accepted 11 June 2025
Available online 19 June 2025

cultivation (Poortenaar et al., 2001). Global production in 2018 was estimated at approximately 3350 tons, primarily driven by Australia with 2600 tons (EUMOFA, 2020). In Europe, three RAS systems produce kingfish including the Netherlands (Kingfish-Company; yearly production (YP) 600 tons per year (t/y)), Denmark/Norway (Nordic-Aquafarms, YP ≈ 900 t/y) and Germany (InfiniteSea-GmbH; YP ≈ 300 t/y)] (EUMOFA, 2020). The species is commonly raised in sea cages and, more recently, in land-based systems (Duman et al., 2022; Orellana et al., 2014; Symonds et al., 2014). The use of Recirculating Aquaculture Systems (RAS) has become crucial in intensive fish production, providing both economic and environmental advantages (Ahmed and Turchini, 2021; Badiola et al., 2012; Dalsgaard et al., 2013). Land-based RAS, in particular, allows for extensive control and manipulation of environmental variables to enhance production efficiency (Timmons et al., 2018). However, the emphasis on water recycling in RAS raises concerns, as maintaining high fish densities may result in the development of suboptimal water conditions (Pan et al., 2020; Summerfelt et al., 2000).

Ensuring high water quality in RAS is essential for preserving fish health and maximizing production, with microbial communities playing a crucial role in both maintaining water quality and impacting fish well-being (Llewellyn et al., 2014; Vadstein et al., 2013, 2018). While certain bacteria have a positive impact on fish health, the presence of pathogenic and opportunistic microbes poses serious threats in closed systems like RAS (Drønen et al., 2022; Netzer et al., 2021). Even non-pathogenic microorganisms, such as sulfate-reducing bacteria (SRB), have the potential to adversely impact fish health by generating toxic H_2S in anaerobic conditions (Alipio et al., 2023; Bergstedt and Skov, 2023; Ciani et al., 2024a; Kiemer et al., 1995). However, the intensification of aquaculture has resulted in an escalation of disease outbreaks from different pathogens including vibriosis and pasteurellosis (Frans et al., 2011; Romalde, 2002; Toranzo et al., 2005; Toranzo, 2004; Zhang et al., 2020). Despite the critical role of microbiota, there is a scarcity of information on its characterization in RAS involving kingfish. While a prior study explored kingfish intestine microbiota in RAS (Ramírez and Romero, 2017), very limited information is available for the microbiota composition in other tissues of this species or different locations within the corresponding RAS.

In addition to microbiota profiling, other methodologies can provide direct information on fish health and the overall quality of the system. Tissue histology plays a crucial role in aquaculture management due to its ability to detect changes before visible symptoms manifest, serving as an effective tool for early issue identification (Wolf, 2018; Wolf et al., 2015). While pure descriptive histology may pose challenges in statistical association with rearing parameters, quantitative and semi-quantitative histopathological scoring systems (Bernet et al., 1999) offer valuable insights into fish health that can be easily linked to rearing parameters (Saraiva et al., 2015, 2016). Semi-quantitative protocols have been applied to different species including Atlantic salmon [*Salmo salar* (Ciani et al., 2024b; Østevik et al., 2021)], turbot [*Scophthalmus maximus* (Saraiva et al., 2016)], gilthead seabream [*Sparus aurata* (Pacorig et al., 2022)] and European seabass [*Dicentrarchus labrax* (Pacorig et al., 2022; Saraiva et al., 2015)]. To the author's knowledge, a semi-quantitative scoring system has been developed only for the liver in kingfish.

This study aimed to conduct a thorough analysis of a commercial RAS farming cycle of *Seriola lalandi*, considering biotic and abiotic parameters indicative for fish health and system quality. First, a detailed microbiota profiling was conducted via 16S rRNA gene amplicon sequencing over different RAS locations (fish tank, denitrification unit, and biofilter) and fish tissues (gills, intestine, and skin). To quantify the presence of potentially pathogenic species like *Vibrio harveyi*, *Vibrio anguillarum*, and *Photobacterium damselae* subspecies *piscicida*, new digital PCR protocols were developed. The study also introduced a semi-quantitative scoring system for gills, intestine, liver, spleen, and kidneys. These parameters were analyzed for a portion of eight months of the production cycle to explore variations over time, associating them with real-time monitoring of chemo-physical water parameters and daily mortality.

2. Material and methods

2.1. Rearing conditions of the recirculating aquaculture system

Yellowtail kingfish (*Seriola lalandi*) were reared at the InfiniteSea GmbH Recirculating Aquaculture System (RAS) in Völklingen, Germany in 2021. Fish were kept in one RAS with two grow-out raceway tanks, with a total volume of 1750 m^3, from 20 g to harvest size (ca. 3 kg). The stocking density was designed to reach 80–85 Kg/m^3 at harvesting size. Fish were fed a commercial diet consisting of *Seriola Protec* 7 mm pellets (Skretting, Spain). The feeding rate was maintained at 1 % of the estimated biomass per day, in accordance with standard aquaculture practices for *Seriola lalandi* at the respective developmental stage. Feed was delivered using an automatic feeding system (Arvotec, Integrated Aqua Systems, USA).

The farm utilized artificial saltwater, with a targeted daily water renewal rate of less than 0.5 %. Seawater was prepared by mixing tap water with a commercial salt mixture (SEEQUASAL Salz Produktion und Handel GmbH, Münster, Germany).The RAS consisted of two drum filters with screen panels of 100 mm and 60 mm (Hydrotech, Velinge, Sweden) and a protein skimmer (Sander, Uetze-Eltze, Germany) to remove large and fine particulate waste, respectively. The protein skimmer operated with ozone (dosing interval between 200 and 300 mV) to enhance the removal of fine solids, reduce bacterial load, and oxidize a portion of the Total Ammonia Nitrogen (TAN) and nitrite. The system also included a Moving Bed Biofilter Reactor (MBBR), a denitrification reactor, a degasser unit, and three propeller pumps for water circulation. The water temperature was regulated through a plate heat exchanger. A Programmable Logic Controller (PLC) was employed to automate circulation pumps, mixing pumps, drum filters running, technical oxygen, sodium hydroxide dosing, acetic acid and ozone dosing. Water parameters were measured in real-time using the Endress+Hauser system (Germany) and included dissolved oxygen (mg/L), pH, redox potential (mV), temperature (°C), conductivity (ms/cm) and H_2S (mg/L). The sensors were placed in the inlet, outlet, and at the center of the fish tank and the denitrification unit. Additionally, total ammonia nitrogen (TAN, Nessler method), nitrite (NO_2^-, diazotization method), nitrate (NO_3^-, cadmium reduction method), phosphate (PO_4^{3-}, amino acid method) and total residual oxidants concentration (TRO, DPD method) were measured using a spectrophotometer (Hach Lange DR2000). Such parameters were collected periodically every 3–4 days at the fish tank inlet. All values are reported in the results section "2.1. Water quality" and in Fig. 1 and Fig. 2. A schematic representation of the system is available in Supplementary fig. 1.

Daily mortality was documented by recording both the number of deceased fish and the dead biomass in Kg. To maintain confidentiality regarding sensitive farm information, mortality is presented here as relative mortality, expressed as the fold-change in dead biomass on any day compared to the dead biomass recorded on a randomly selected date (January 1st).

2.2. Microbiota profiling in fish and RAS samples

Microbial community compositions were identified via 16S rRNA gene amplicon sequencing.

2.2.1. Sample collection and DNA isolation

Samples were collected in triplicates once a month at nine distinct time points (April to December 2021), amounting to a total of 262 samples. All samples were collected and processed individually. Prior to sampling, fish were fasted for 12 h. The sample set included swabs of tank biofilm (TB), biofilter biofilm (B) and biofilter carrier (BC),

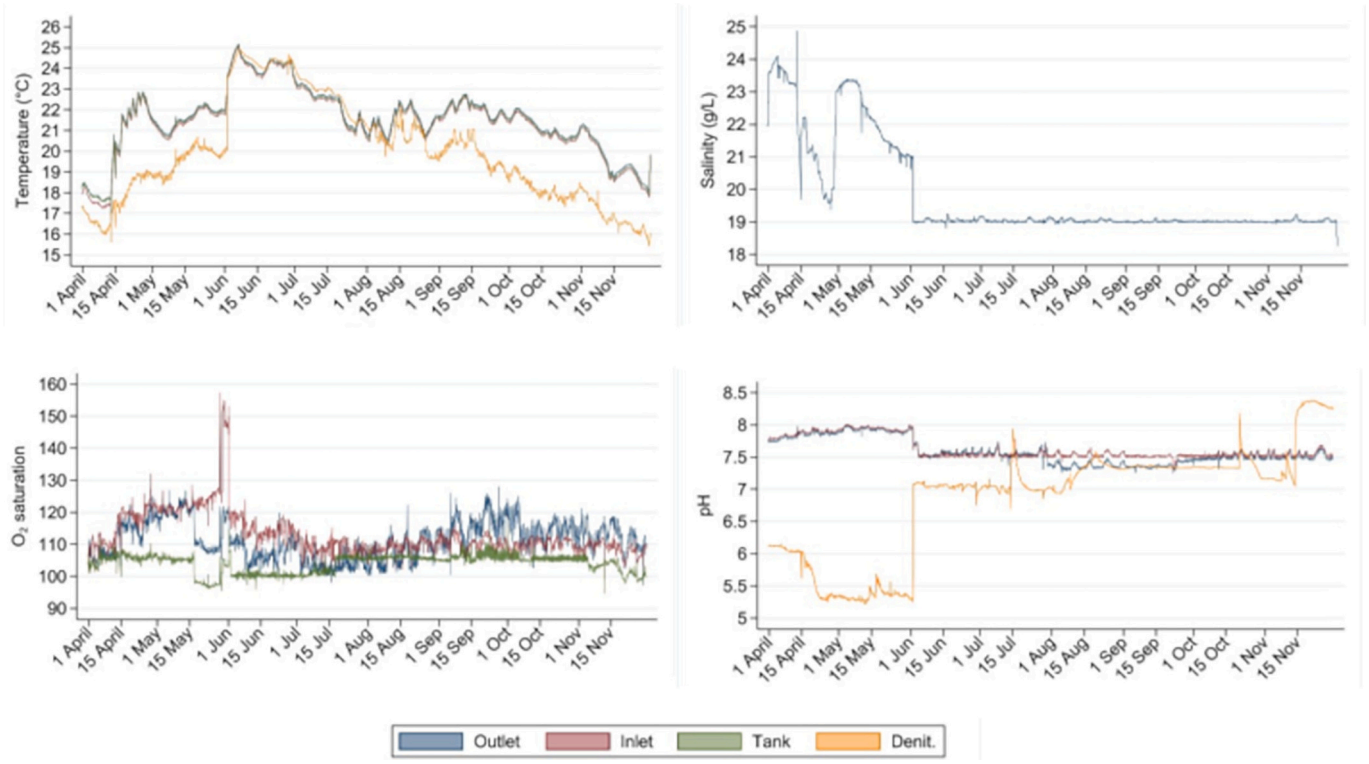

Fig. 1. Chemo-physical water parameters. The values are shown for the sampling period from April to November 2021. The sensors were located before the tank (Inlet) in the center of the tank (Tank) just outside the tank (Outlet) and in the denitrification unit (Denit.)

together with water samples from the fish tank (TW) and denitrification unit (D).Swabs of mucus samples were collected from the intestine (GUM), skin (SKM), and gill (GIM). Additionally tissue excisions of intestine (GUM2) were collected excluding fecal matter. The two groups of samples are defined either as "RAS samples" or "Fish samples" throughout the manuscript. Swab of biofilm and mucus samples were collected using the DNA/RNA Shield Lysis Tubes w/Swab (microbe)-kit (Zymo Research, USA) according to the manufacturer's protocol. For liquid samples, 200 mL water was filtered through 0.22 μm Sterivex filters (Merck Millipore, Germany). Residual water was removed by pushing air through the filter cartridge before adding 2 mL DNA/RNA-Shield (Zymo Research, USA). The cartridges were stored at 4 °C until further processing. Filter membranes were manually removed from the filter cartridges, cut into small pieces and used for total DNA extraction.

DNA isolation was conducted using the ZymoBIOMICS DNA Miniprep Kit (Zymo Research, USA) in combination with the FastPrep24 instrument (MP Biomedicals, USA). The same metagenomic DNA samples were used for 16S rRNA gene amplicon sequencing and digital PCR (dPCR) monitoring of pathogenic species (See chapter 1.4).

2.2.2. 16S rRNA amplicon library preparation and Illumina MiSeq sequencing

The preparation of the amplicon sequencing library adhered to the "16S rRNA Metagenomic Sequencing Library Preparation" protocol from Illumina Inc. (San Diego, CA, USA) applying 16S rRNA gene V3-V4 universal primers Pro341F (5'-CCTACGGGNBGCASCAG-3′) and Pro805R (5'-GACTACNVGGGTATCTAATCC-3′) (Takahashi et al., 2014). Subsequently, the 16S rRNA gene amplicon libraries were subjected to sequencing on the Illumina MiSeq platform, employing the protocol for 2 × 300 bp paired-end reads.

2.2.3. Bioinformatic processing, diversity analyses and visualization of results

2.2.3.1. Bioinformatic processing involved two in-house pipelines. The initial pipeline handled the pre-processing of sequencing reads, including tasks such as merging forward and reverse reads using FLASH (Magoč and Salzberg, 2011), primer removal with Cutadapt (Martin, 2011), trimming reads based on quality with Sickle (Joshi and Fass, 2011), and conducting quality control for high-quality (HQ) sequences using FastQC (Andrews, 2010).

Subsequent processing steps were conducted within the second pipeline, specifically designed for analyses within the QIIME2 platform (Bolyen et al., 2019). The datasets underwent denoising using DADA2 (Callahan et al., 2016), alignment of amplicon sequence variants (ASVs) with Mafft (Katoh et al., 2002), and calculation of unrooted and rooted phylogenetic trees using Fasttree (Price et al., 2010). Taxonomic assignment of amplicon sequences was performed using q2-feature-classifier (Bokulich et al., 2018) Classify-Sklearn (Pedregosa et al., 2011) against the Silva database release 138, (Quast et al., 2013). The datasets underwent filtering to exclude eukaryotic sequences, ASVs with frequencies below five, and were rarefied to a specified depth of 20,000 sequences, which yielded 224 samples that met the quality criteria.

The normalized taxonomic profiling tables were represented as bar charts, Bray-Curtis dissimilarity matrices, tree diagrams and ordination plots. All statistical analyses were performed using R-Studio Statistical Software v2024.12.1 (R Core Team, 2024).

2.3. Digital PCR (dPCR) for pathogen detection in fish and RAS samples

2.3.1. Pathogen selection

The selection of pathogens for investigation via dPCR was based on InfiniteSea's previous research, highlighting *Vibrio harveyi*, *Vibrio anguillarum*, and *Photobacterium damselae* subspecies *piscicida* as the pathogens of greatest operational interest being previously detected in

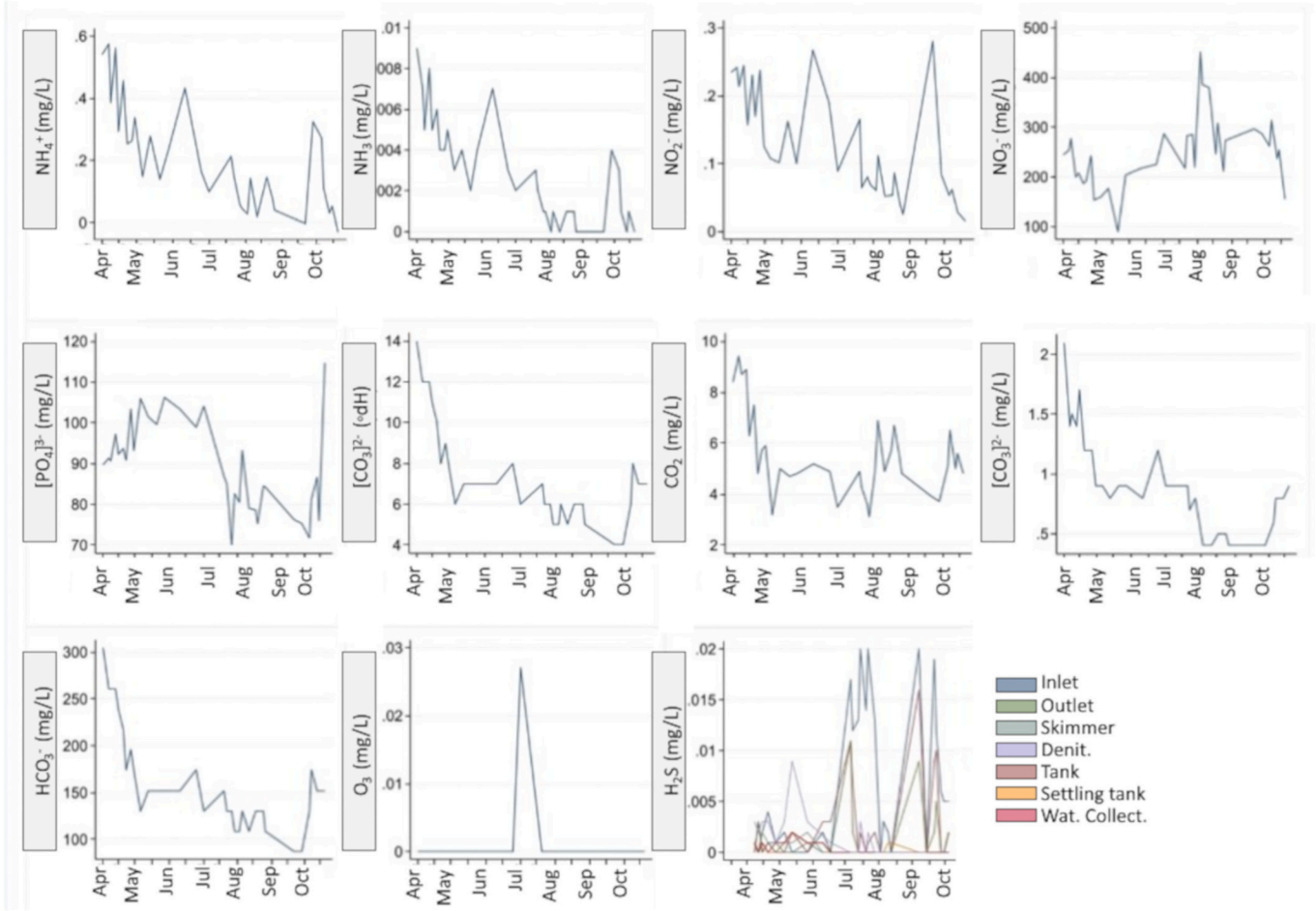

Fig. 2. Solutes concentrations in RAS water plotted against the sampling time frame (Apr. - Nov. 2021). All parameters were collected by sensors located in the inlet of the fish tank. Dissolved hydrogen sulfide (H_2S) was additionally measured in the outlet and center of the fish tank, as well as the protein skimmer, denitrification unit, settling tank and water collector. NH_4^+ ammonium; NH_3 ammonia, NO_2^- nitrite; NO_3^- nitrate; PO_4^{3-} phosphate; CO_3^{2-}carbonate; CO_2 carbon dioxide; HCO_3^- bicarbonate; O_3 ozone; H_2S hydrogen sulfide.

both production environment and fish intestine. Reference DNA samples of these bacteria were supplied by the University of Patras. *Vibrio anguillarum* strain LMG 4437, was isolated from Atlantic cod (*Gadus morhua* L.) by Dr. J. Bagge (Makridis et al., 2021); *Vibrio harveyi* strain VH2, was isolated from farmed juvenile *Seriola dumerili* during outbreaks of vibriosis in Crete, Greece (Castillo et al., 2015), and *Photobacterium damselae* subspecies *piscicida*, strain OP, was isolated from gilthead seabream and gently provided by Dr. P. Katharios from the Hellenic Center for Marine Research, Heraklion, Crete, Greece.

2.3.2. Primer design

Primers (Table 1) for the dPCR were created by modifying Real-Time PCR (qPCR) protocols found in existing literature or designing primer/probe combinations with Primer3 software (Untergrasser et al., 2012) using nucleotide sequences of the corresponding three pathogenic bacteria accessible at NCBI). Eurofins Genomics synthesized the oligonucleotide primers and TaqMan™ probes in HPLC-grade quality.

The specificity and efficiency of the primers were tested using DNA from the three selected bacteria as a template for dPCR assays. The DNA of these bacteria were supplied by the University of Patras.

2.3.3. dPCR assay protocol

DNA extracted (See chapter 1.3.1) from fish tank water (TW), biofilter biofilm (B), denitrification units (D) and segments of the intestinal mucosa (GUM2), was chosen for subsequent analysis using dPCR. One sample per location per time point from May to December, except for

Table 1
Sequences of primer and TaqMan probe oligonucleotides, corresponding target microbe. [1] Own work; [2] (Fukui and Sawabe, 2008).

Species	Primer/Probe ID	Sequence 5′ → 3’	Target	Accession number
Vibrio anguillarum [1]	Fw	GGTGCTTCTTCTGTCGCTAA	*16S rRNA*	MK967051.1
	Rev	AGGCCTTCGGGTTGTAAAG		
	Probe (CY5)	AACAACACCACCTTCCTCACGACT		
Vibrio harveyi [2]	Fw	CGAGCGGAAACGAGTTATCTG	*16S rRNA*	MT605270.1
	Rev	CTCACCAACTAGCTAATCCCACCTA		
	Probe (CY3)	CCGCATAATACCTACGGGTCAAAGAGGG		
Photobacterium damselae ssp. *piscicida* [1]	Fw	TGCTGGTGGTGTATTCTGGG	*phdP*	AY191100
	Rev	GCGATTGCTTGTTGCCATAAC		
	Probe (HEX)	CGGACGTTTAGCTGGTGCTCTGA		

July and October, was included in the assessment. The dPCR process was initiated by preparing 25 μL reaction mixtures, which included 1× concentrated PerFecTa Multiplex qPCR ToughMix (Quanta Biosciences, Gaithersburg, MD, USA), 1 μM fluorescein (Saint Louis, MO, USA), 10 μM primers, 5 μM corresponding TaqMan probe, and an appropriate amount of DNA template (5–280 ng/μL total DNA). Subsequently, four PCR reaction mixtures of 25 μL each were loaded onto a Sapphire chip and inserted into the Naica Geode instrument to partition into 15,000 to 30,000 droplets and undergo PCR amplification. The applied PCR conditions included an initial step of 5 min at 95 °C, followed by 40 cycles of 1 min at 95 °C and 30 s at 60 °C, with a final holding step at 4 °C. Sapphire chips were then transferred to the Naica Prism3 fluorescence reader for imaging. Data analysis was carried out using Crystal Miner software V2.3.5 (Stilla Technologies). To control for DNA contamination, reactions with no template (NTC) were included for all assays. Additionally, the results, represented as target gene copy numbers, were normalized for 1 ng DNA, yielding the unit copies per ng of extracted total DNA.

2.4. Fish histopathology analyses

2.4.1. Fish samples preparation

Monthly collections were conducted from April to November 2021, with three fish sampled at each time point. Tissues, including liver, spleen, kidney, and anterior intestine, were collected at all time points, while gills were additionally collected during the last two samplings in October and November.

Euthanasia was carried out by placing the fish in a 200 L tank with 150 mg/L of MS-222 (tricaine methanesulfonate), followed by dissection, isolation and fixation of tissues in a 4 % formaldehyde Phosphate Buffered Solution (PBS). In the laboratory, samples underwent a one-hour immersion in distilled water, followed by dehydration in sequential ethanol solutions of 70 %, 80 %, and 100 %. Subsequently, tissues were treated with Technovit and absolute ethanol for one hour each and embedded in Technovit for 24 h.

Serial 5 mm sections were obtained using a Leica SM2000R microtome (Germany) and stained with a combination of methylene blue (Sigma, Germany), azure II (Sigma, Germany), and basic fuchsin (Polysciences, USA) following a previously published protocol (Bernet et al., 1999). At least six different slides per sample were analyzed. Observations were conducted using a light microscope (Zeiss AX10 Image A2), and all measurements were processed with ImageJ software (Schneider et al., 2012).

2.4.2. Fish tissue histopathological scoring system

A Multiparametric Semi-Quantitative Scoring System (MSSS) was adjusted from a previous publication (Pacorig et al., 2022) to assess tissue pathology. MSSS incorporates 27 parameters associated with five organs (Table 2).

These parameters were selected for their sensitivity to rearing conditions, water quality factors (temperature, salinity, protozoan abundance), nutrition, stress, and bacterial or parasite infections, serving as indicators of the overall health status of the fish. The MSSS scoring ranges from 0 to 5, where 0 indicates the absence of the damage, and 5 represents the maximum extent of the evaluated damage (Table 3). Indices were assessed on six different tissue slides using ImageJ software based on one of three criteria: i) **Number** – Goblet cells, inflammatory cells, and ectoparasites were counted, and the index was scored accordingly. ii) **Extension** – Undifferentiated areas, hyperemia, vacuolar degeneration, multifocal glycogen accumulation, nephrocalcinosis, multifocal exudates, melanomacrophage centers, and necrosis were quantitatively assessed based on the percentage of surface area occupied.

iii) **Qualitative description** – Chloride cell hypertrophy, clubbing, hyperplasia, basal fusion, and edema of the secondary lamellae in the gills were evaluated qualitatively using descriptive criteria summarized in Table 3.

3. Results

3.1. Water quality

In early June, adjustments were made to manage water parameters, as evident in Fig. 1, particularly in temperature, pH, O_2 saturation, and salinity. These parameters exhibited higher daily and weekly variations in April and May but were subsequently stabilized with minimal fluctuations afterwards. For example, salinity measured at the fish tank outlet ranged from 19.5 to 24 g/L in May and June, before being fixed at 19 g/L from July onward. The pH in both the inlet and outlet varied between 7.7 and 8.0 in May and June and was then stabilized at 7.5 from July onward. In the denitrification unit, pH fluctuated between 5.4 and 6.2 in May and June, stabilized at 7 between June and mid-August, and slightly increased from 7.0 to 7.5 from mid-August to mid-November, peaking at around 8.3 thereafter. The water temperature at the center of the fish tank rose from 18.0 to 25.0 °C from April to mid-June, gradually decreasing afterwards and stabilizing between 20.5 and 23.0 °C from August to November. Temperature exhibited relative stability during the day and changed gradually over the days and weeks.

Various additional parameters were assessed in the inlet water, as illustrated in Fig. 2, focusing on nitrogen and carbon compounds. Such measurements indicated that ammonium (NH_4^+) remained <0.6 mg/L, ammonia (NH_3) < 0.01 mg/L, nitrite (NO_2^-) < 0.3 mg/L, and nitrate (NO_3^-) < 450 mg/L. Despite daily fluctuations, all values exhibited a declining trend over time, except for nitrate, which increased. Carbon compounds displayed a similar trend, with peak values observed at the beginning of April and subsequent decreases leading to relatively stable levels from May onward. Carbon dioxide (CO_2) consistently remained <10 mg/L, Carbonate (CO_3^{2-}) < 2.5 mg/L, and bicarbonate (HCO_3^-) < 300 mg/L.

Ozone (O_3) was never detected, except at one time point on July 1st with a concentration below 0.03 mg/L (Fig. 2).

Hidrogen sulfide (H_2S) (Fig. 2) consistently remained <0.02 mg/L across all measured locations, including the inlet, outlet, and center of the fish tank, as well as the skimmer, denitrification unit, water collector, and settling tank.

Table 2
List of histopathological parameters evaluated in the different tissues.

Gills	Intestine	Liver	Spleen	Kidney
Chloride cell hypertrophy	Goblet cells	Lipid	Multifocal exudates	Nephrocalcinosis
Clubbing of sec. Lam.	Inflammatory infiltrates	Hyperemia	Melanomacrophage	Inflammatory infiltrates
Hyperplasia of sec. Lam.	Desquamation	Vacuolar degeneration	Necrosis	Vacuolar degeneration
Basal fusion of sec. Lam.	Myxosporidia	Multifocal glycogen accumulation	Undifferentiated areas	Hyperemia
Oedema		Necrosis		Necrosis
Goblet cells				Melanomacrophage
Inflammatory infiltrates				
Ectoparasites				

Table 3
Histopathological scoring system. Each parameter was scored on a scale from 0 to 5, based either on the number of observed lesions, the extension or its qualitative evaluation across six different slides per tissue.

Goblet cells		
Score	Description	Number
0	Absent	0
1	Very scarce	1 to 5
2	Scarce	6 to 20
3	Moderate	21 to 40
4	Abundant	41 to 60
5	Highly abundant	>60
Inflammatory cells		
Score	Description	Number
0	Absent	0
1	Very scarce	1 to 5
2	Scarce	6 to 20
3	Moderate	21 to 50
4	Abundant	51 to 150
5	Highly abundant	>150
Ectoparasites, Myxosporidia		
Score	Description	Number
0	Absent	0
1	Very scarce	1
2	Scarce	2 to 3
3	Moderate	4 to 6
4	Abundant	7 to 9
5	Highly abundant	>10
Undifferentiated areas, hyperemia, vacuolar degeneration, multifocal glycogen accumulation, nephrocalcinosis, multifocal exudates, melanomacrophage centers, and necrosis		
Score	Description	Percentage
0	Absent	0 %
1	Very scarce	<5 %
2	Scarce	5 to 10 %
3	Moderate	11 to 15 %
4	Abundant	16 to 20 %
5	Highly abundant	>20 %
Lipid accumulation in the liver		
Score	Description	Percentage
0	Absent	0 %
1	Very scarce	<10 %
2	Scarce	11 to 25 %
3	Moderate	26 to 40 %
4	Abundant	41 to 55 %
5	Highly abundant	>55 %
Chloride cells hypertrophy		
Score	Description	Definition
0	Absent	Normal condition
1	Very scarce	Slightly hypertrophic cells
2	Scarce	Hypertrophic cells but not proliferated along the secondary lamellae
3	Moderate	Hypertrophic cells, which begin to proliferate along the secondary lamellae
4	Abundant	Hypertrophic cells proliferation along the secondary lamellae
5	Highly abundant	Hypertrophic cells with severe proliferation and alteration of the structure of the secondary lamellae
Clubbing, hyperplasia, basal fusion, and oedema of the secondary lamellae		
Score	Description	Definition
0	Absent	Normal condition
1	Very scarce	Slightly appearance in the secondary lamellae
2	Scarce	Appearance, which does not affect the shape of the secondary lamellae
3	Moderate	Appearance, which begins to affect the shape of the secondary lamellae
4	Abundant	Appearance, which affects the shape of the secondary lamellae
5	Highly abundant	Severe appearance, which alters completely the shape of the secondary lamellae
Desquamation		
Score	Description	Definition
0	Absent	No detached cells from the epithelium
1	Very scarce	Very few cells in detachment process
2	Scarce	Few cells in detachment process
3	Moderate	Detached cells in the lumen, no alteration of the epithelium
4	Abundant	Detached cells in the lumen, altering ≤50 % of the epithelium
5	Highly abundant	Detached cells in the lumen, altering >50 % of the epithelium

3.2. Microbiota profiles of fish tissues and RAS samples

At the domain level, the majority of 16S rRNA gene sequences were attributed to *Bacteria* (25.5–100 %), with a minority assigned to *Archaea* (0–14.8 %), while 0 up to 74.3 % remained unassigned.

Various bacterial phyla were identified in the analyzed samples (Supplementary fig. 2). In the RAS samples, the predominant bacterial phyla were *Proteobacteria* (28.6–98.5 %), *Bacteroidota* (0.7–39.3 %), *Actinobacteriota* (0.04–26.9 %), and *Nitrospirota* (0–23.7 %). Among the archaeal phyla, *Crenarchaeota* (0–14.8 %) was the most abundant. In the fish samples, *Proteobacteria* (2.1–97.7 %) also dominated the bacterial phyla, followed by *Firmicutes* (0–89.6 %) and *Campylobacterota* (0–66.5 %). *Nanoarchaeota* (0–13.2 %) emerged as the most abundant archaeal phylum within the fish samples.

At the genus level (Fig. 3), the RAS samples exhibited *Erythrobacter* (up to 57.0 %), *Glaciecola* (up to 41.0 %), and *Nitrospira* (up to 23.7 %) as the most prevalent genera. In the fish samples, *Aliivibrio* (up to 79.8 %), *Pseudomonas* (up to 75.4 %), and an uncultured genus from the family *Mycoplasmataceae* (up to 73.1 %) were identified as the predominant genera. However, on the genus level a large proportion of microbial communities remained unassigned.

The clustering of taxonomic profiles from the 226 RAS and fish samples (Fig. 3) showed that the nine identified clusters could be categorized into two main sections. The first section (Cluster I-III) included all RAS samples, along with some skin (SKM) and gill (GIM) samples. The second section (Cluster IV to IX) contained all remaining fish samples. Cluster I (yellow) was formed by 31 samples (15 TW, 8 SKM, 8 GIM). Cluster II (red) stands out as the largest cluster, comprising 100 samples (24 TB, 21 B, 24 BCE, 24 D, 4 SKM, 3 GIM). Within this cluster, distinct subclusters corresponded to different sampling sites (e.g., TB, B, BC, D), while the seven fish samples were dispersed within the cluster. Cluster III (blue) contained 18 samples (9 TW, 1 SKM, 8 GIM), with the TW and fish samples forming two separate subclusters. Cluster IV (cyan) included five fish samples (2 SKM, 3 GUM), acting as a transitional group between the two major sections of the tree diagram. Cluster V (orange) comprised 26 fish samples (11 SKM, 10 GIM, 5 GUM), while cluster VI (light brown) was composed of nine fish samples (3 GIM, 6 SKM). Cluster VII (light blue) included 11 fish samples (5 SKM, 2 GIM, 4 GUM). Cluster VIII (grey) consisted of 14 GUM samples, and cluster IX (green) included 10 GUM samples.

Each of these clusters exhibited a characteristic composition in terms of genera (Fig. 4). Among the identified clusters, Clusters I, IV, V VII and IX had a dominant genus with a relative abundance exceeding 25 % (I-*Erythrobacter* 38 %; IV *Escherichia-Shigella* 31 %; V *Pseudomonas* 35 %; VII *Anaerobacillus* 27 %; IX *Vibrio*, 38 %). In contrast, the remaining clusters exhibited a more diverse microbial composition, with multiple genera present at lower relative abundances. For instance, in clusters II, III, VI and VIII the most abundant genera ranged between 4 % and 8 % (II *Nitrospira* 8 %; III *Erythrobacter* 6 %; VI *Pseudomonas* 5 %; VIII *Vibrio* 4 %).

The taxonomic profiles of RAS samples were subjected to nonmetric multidimensional scaling (NMDS) analysis (Fig. 5). The NMDS of tank water samples (Fig. 5B) revealed three distinct clustering of samples

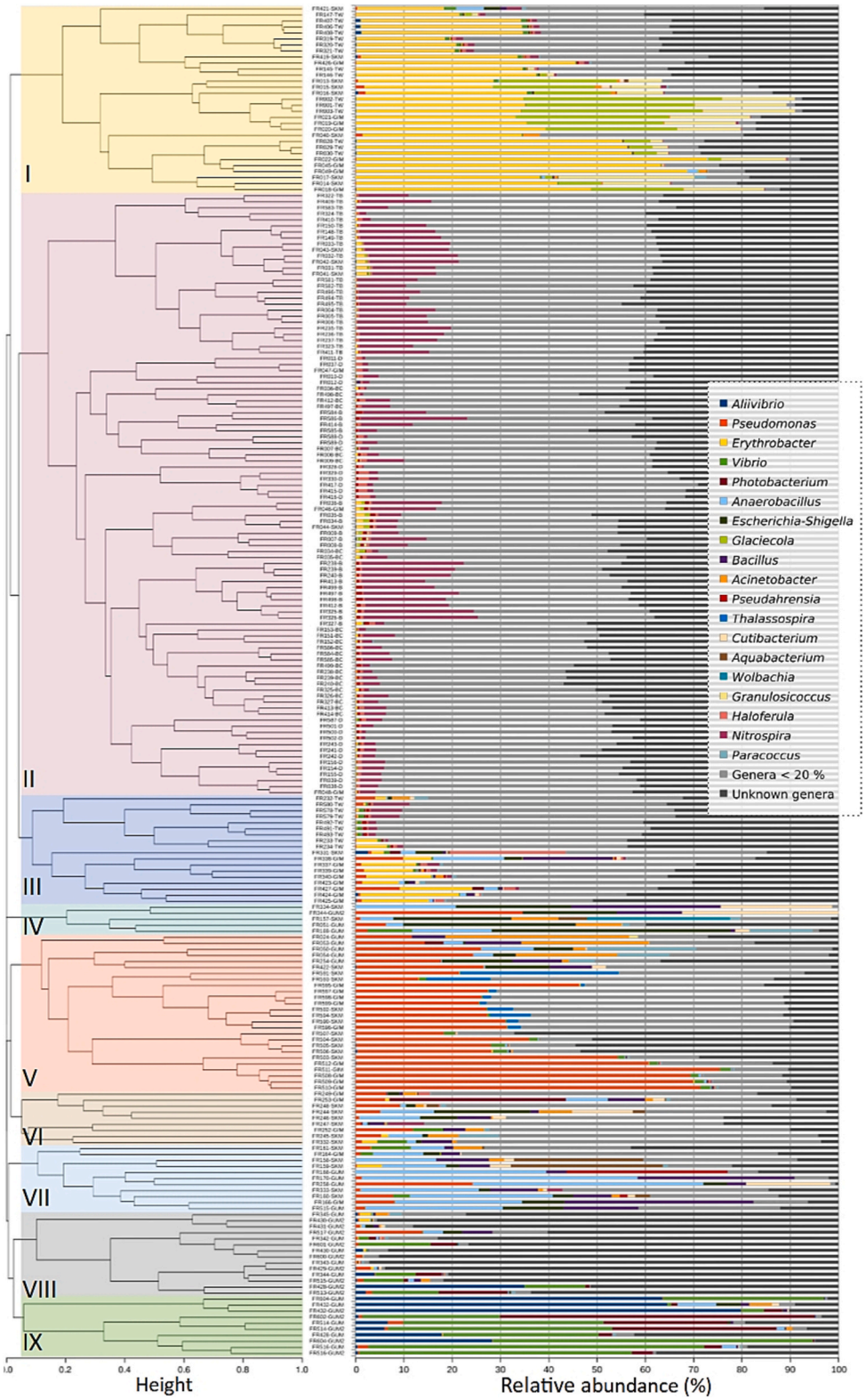

Fig. 3. Clustered (Bray-Curtis distances) taxonomic profiles on genus level of RAS and fish samples based on 16S rRNA gene amplicon sequencing. Nine clusters formed and were indicated by Latin numerals from I to IX. (TW) tank water; (TB) tank biofilm; (B) biofilter biofilm; (BC) biofilter carrier; (D) denitrification unit; (GUM) intestine mucus; (SKM) skin mucus; (GIM) gill mucus. Not all sample names are shown due to space limitations. Genera with a maximal relative abundance below 20 % were summarized and the proportion of taxa, which were unknown on the genus level are shown in dark grey.

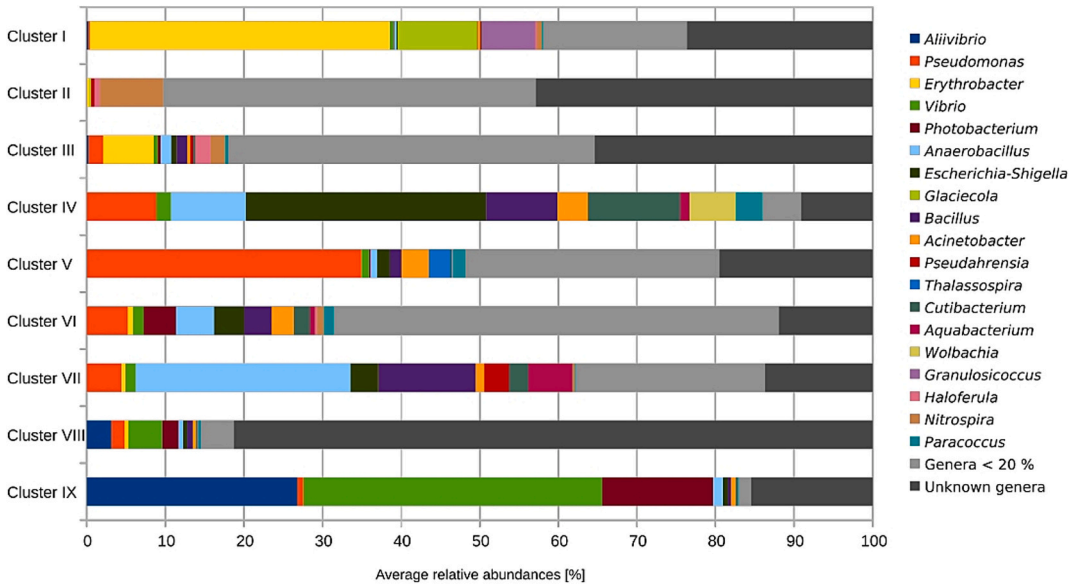

Fig. 4. Bar chart displays the average abundances of the most prevalent taxa within the taxonomic profiles of 226 samples, categorized into nine clusters. Clusters were revealed based on Bray-Curtis distances calculated in R. Genera representing 20 % or more of the relative abundance in at least one of the clusters are identified using different color codes. Genera below this threshold are grouped together and represented by grey bars. Unknown genera are represented by dark grey bars.

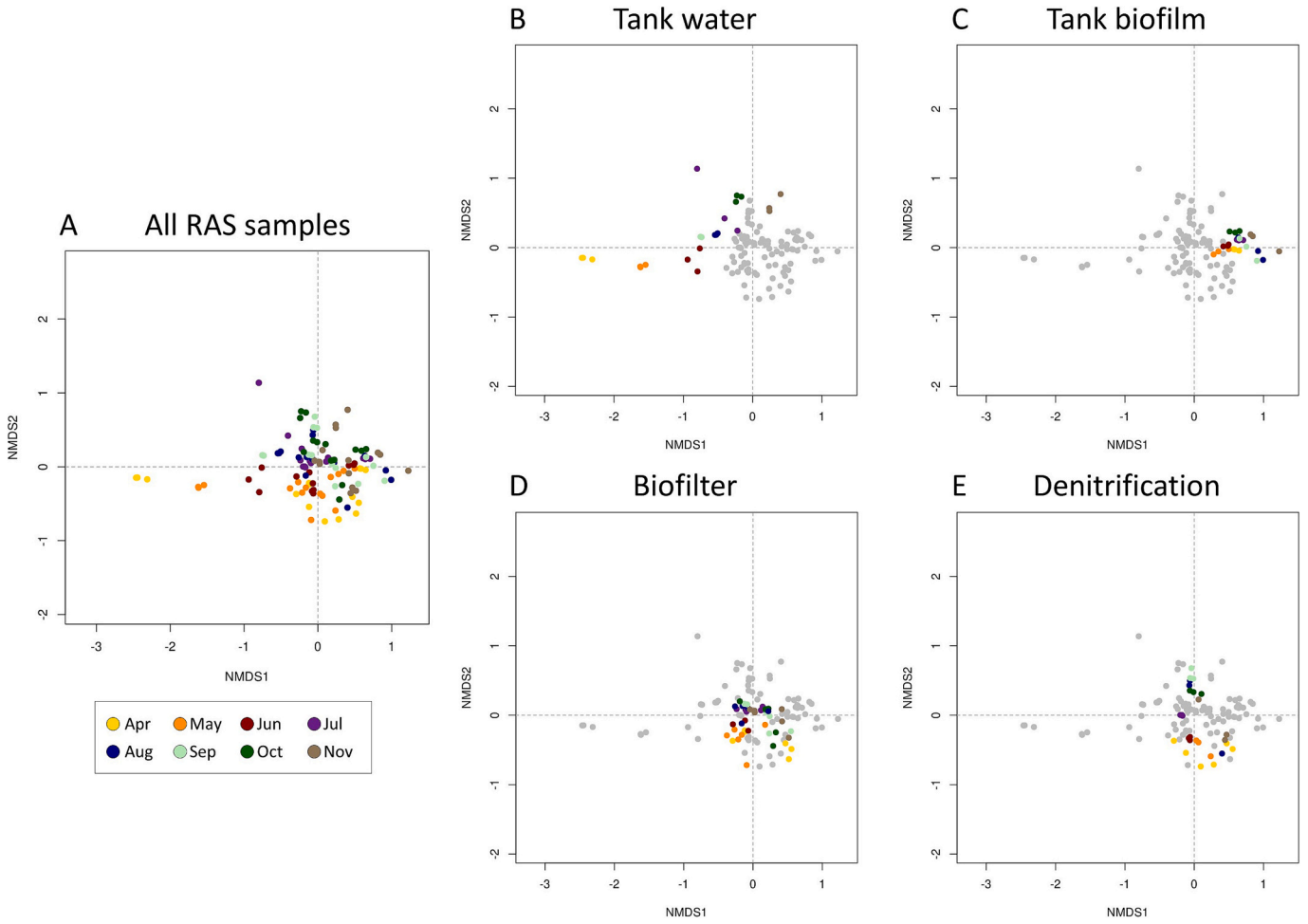

Fig. 5. Nonmetric multidimensional scaling (NMDS) of the taxonomic profiles of RAS samples using Bray-Curtis distances calculated in R. The results are presented with color-coding corresponding to the sampling time points. In fig. (A), samples from the different locations are displayed collectively. Additionally, Figs. B-E highlight either tank water (B), tank biofilm (C), biofilter (D) and the denitrification unit (E) while keeping different samples in grey.

according to the time points in April, May, and June–November. Notably, from June onwards, the distances between replicates from different time points decreased. All other RAS sampling locations (tank biofilm; biofilter and denitrification units) exhibited no variation over time, forming a single main cluster (Fig. 5C-D-E).

Fish samples were also subjected to NMDS analysis (Fig. 6). Both gills (Fig. 6B) and skin (Fig. 6C) samples showed time-based clustering of April and May samples as compared to later time points. Such overtime variations were less evident in intestine samples (Fig. 6C-D).

3.3. Detection of potential fish pathogens with dPCR

The presence of the three potential pathogens was monitored over time in different RAS locations and in intestine microbiota with a dPCR approach (Fig. 7).

The presence of *P. damselae piscicida* was almost negligible in the biofilter, denitrification unit, tank biofilm and intestine mucosa. It was identified in the tank water, exhibiting concentrations ranging from 1 to 1.8 copies/ng total DNA (cp/ng) during the period from May to December. A peak concentration of around 7 cp/ng was noted in August, while it was not detected in November.

The level of *Vibrio harveyi* in tank water was variable, ranging from around 1 cp/ng in May and June to 2–4 cp/ng in August and September, respectively. Subsequently, it was not detected in November and December. *Vibrio harveyi* was absent in the denitrification except for a peak in December (approximately 17 cp/ng). A minor presence was identified in the biofilter in May (approximately 2.2 cp/ng) and December (approximately 3.8 cp/ng). Notably, *Vibrio harveyi* was absent in the intestine mucosa.

Vibrio anguillarum was identified in tank water, showing a concentration of around 8 cp/ng in May and June, increasing to 38 cp/ng in August and 54 cp/ng in September. It was absent in November but reappeared in December at around 5 cp/ng. In the denitrification unit, *V. anguillarum* showed variable presence, with concentration below 2 cp/ng in May and November, rising to 32–38-cp/ng in June and September, and peaking at 204 cp/ng in December. It was not detected in August. This bacterium was absent in the intestine microbiota at all time points, except in December (approximately 7 cp/ng). In the biofilter, higher concentrations were observed in May (approximately 10 cp/ng), followed by a steady decline from June (approximately 3.5 cp/ng) to November (approximately 0.5 cp/ng), with a second peak in December (approximately 10 cp/ng).

3.4. Histopathological observations in different fish tissues

Fish tissue damage was detected to a different extent across all analyzed tissues and parameters (Fig. 8). Some histopathological parameters exhibited variation over time (Fig. 9). Except for the gills, no variation between biological replicates was observed when grouping different parameters over time. Hence, no statistical tests were

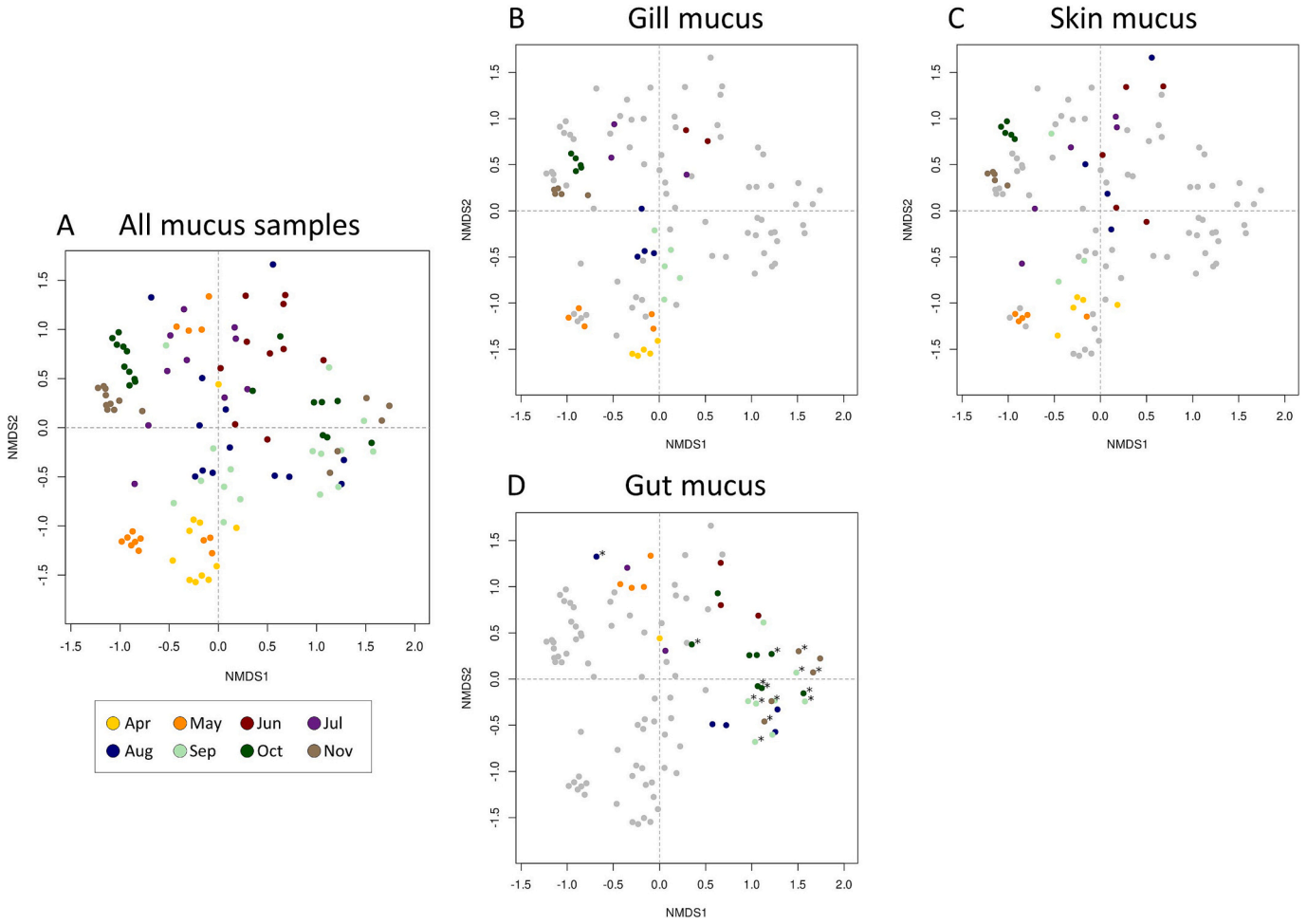

Fig. 6. Nonmetric multidimensional scaling (NMDS) of the taxonomic profiles of fish samples using Bray-Curtis distances calculated in R. The results are presented with color-coding corresponding to the sampling time points. Samples not belonging to the corresponding mucus type are kept in grey (B—D). In the first figure, samples from different locations are displayed collectively (A). Additionally, Figs. B—D provide individual representations for gill (B), skin (C) and intestine (D) mucus. Intestine mucus samples were collected either by tissue swabs (*) or by tissue excisions.

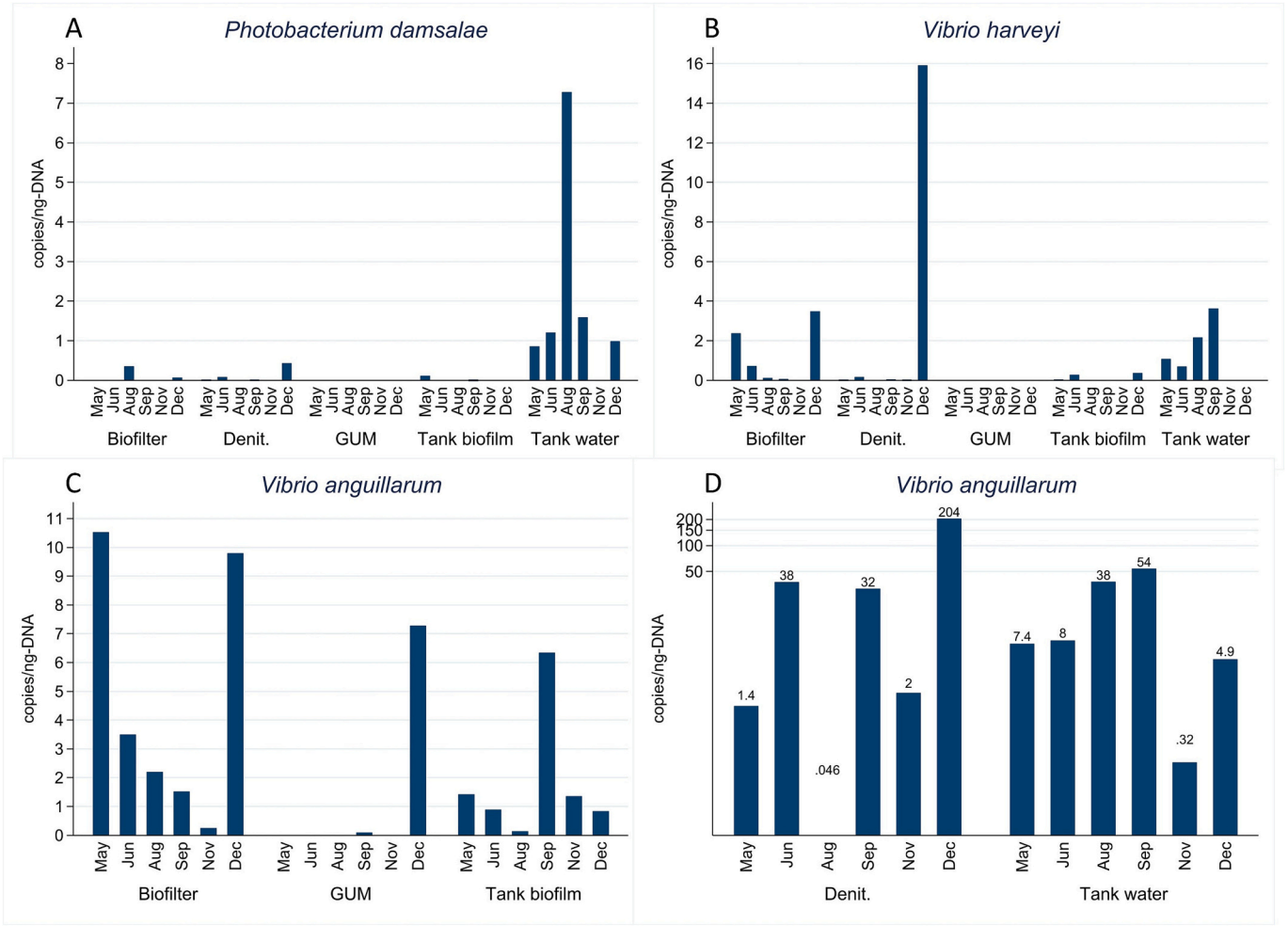

Fig. 7. Monthly quantification (from May to December 2021, excluding July and October) of three potentially pathogenic species: *Photobacterium damselae* (A), *Vibrio harveyi* (B) and *Vibrio anguillarum* (C—D)] in different locations [biofilter, denitrification unit, intestine microbiota (GUM) tank water/biofilm and denitrification unit]. The presence of each species is quantified via a dPCR approach as the number of target DNA copies per ng of isolated DNA from each sample. Note that graph (D) is in logarithmic scale showing the exact concentration above each column to improve clarity.

performed. The histopathological observations for the individual tissues are described in the following paragraphs.

3.4.1. Gills

When considering all biological replicates collected, mean scores (± SD) for gills histopathological parameters were as follows: chloride cell hypertrophy 2.8 ± 0.4; clubbing of secondary lamellae 3.5 ± 0.5; hyperplasia 1.2 ± 0.4; basal fusion of secondary lamellae 1.3 ± 0.5; oedema 1.3 ± 0.5; goblet cells 2.7 ± 0.5; inflammatory infiltrates 3.0 ± 0.0 ectoparasites 1.3 ± 0.5 (Fig. 8).

Gill samples were collected in only two time points (October and November) showing no variation in the different histopathological parameters over time (Fig. 9).

3.4.2. Intestine

When considering all biological replicates collected, mean scores (± SD) for intestine histopathological parameters were as follows: goblet cells 3.0 ± 0.7; inflammatory infiltrates 2.3 ± 1.4; desquamation 2.1 ± 0.3; myxosporidia Not Detected (ND) (Fig. 8).

The scores for goblet cells showed variation over time, starting with minimum values of 2 in April and May, which then increased to 4 in July and August and stabilized at 3 from September to November. Inflammatory infiltrates exhibited minimum scores of 1 from April to July, subsequently rising to 4 from September to November. Desquamation maintained a score of 2 at all time points except for June, where all samples received a score of 3. Myxosporidia was never detected (score 0) in any of the samples at any time point (Fig. 9).

3.4.3. Liver

When considering all biological replicates collected, mean scores (± SD) for liver histopathological parameters were as follows: lipids 3.3 ± 0.5; hyperemia 2.4 ± 0.7; vacuolar degeneration 1.1 ± 0.3; multifocal glycogen accumulation 1.6 ± 0.5; necrosis 2.1 ± 0.3; (Fig. 8).

Hyperemia gradually increased, starting with a score of 2 in April and May, then rising from June to reach its peak at 4 in July. It then decreased to 2.3 in August before stabilizing at 2 afterwards. No variations were observed in the other liver histopathological parameters over time (Fig. 9).

3.4.4. Spleen

When considering all biological replicates collected, mean scores (± SD) for spleen histopathological parameters were as follows: multifocal exudates 2.8 ± 0.54; melanomacrophages 3.7 ± 0.5; necrosis 1.8 ± 0.7; undifferentiated areas 1 ± 0.0 (Fig. 8).

All spleen histopathological parameters showed no variations over time (Fig. 9).

3.4.5. Kidney

When considering all biological replicates collected, mean scores (± SD) for kidney histopathological parameters were as follows:

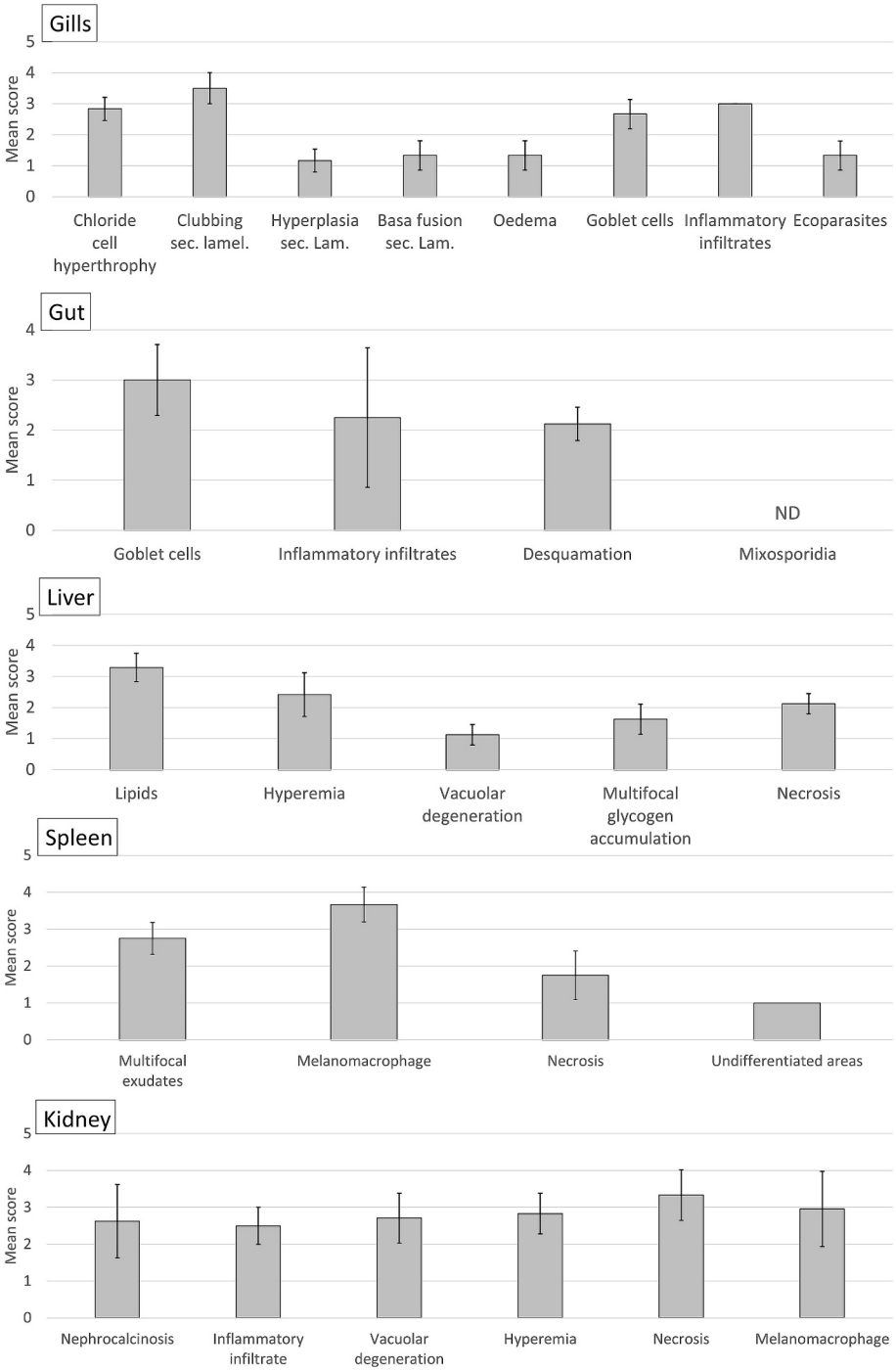

Fig. 8. Fish tissue histopathological scoring system mean scores (±SD) for each analyzed organ and histopathological parameter calculated from all the biological replicates collected (gills $n = 6$; other tissues $n = 24$). ND: Not Detected.

nephrocalcinosis 2.6 ± 1.0; inflammatory infiltrates 2.5 ± 0.5; vacuolar degeneration 2.7 ± 0.7; hyperemia 2.8 ± 0.6; necrosis 3.3 ± 0.7; melanomacrophages 3.0 ± 1.0 (Fig. 8).

Several histopathological parameters exhibited variations over time. Melanomacrophages began with a score of 1 in April, rising to a score of 3 from May to November, with an exception in August where the score peaked at 5. Nephrocalcinosis initiated with a score of 1 in April and increased to scores between 2 and 3 from May to September. The score then escalated to 4 in October and November. Inflammatory infiltrates alternated between scores of 2 and 3 throughout the sampling period (Fig. 9).

3.5. *Relative fish mortality*

Relative fish mortality rates exhibited a consistent decline over time (Fig. 10). The highest peaks were observed during the initial two weeks of April, followed by a subsequent decrease to intermediate levels between mid-April and mid-June, characterized by daily fluctuations. After mid-June, there was a further decline, frequently reaching null values from October onward, with minimal daily fluctuations.

4. Discussion

This study conducted a thorough analysis of an 8-month period

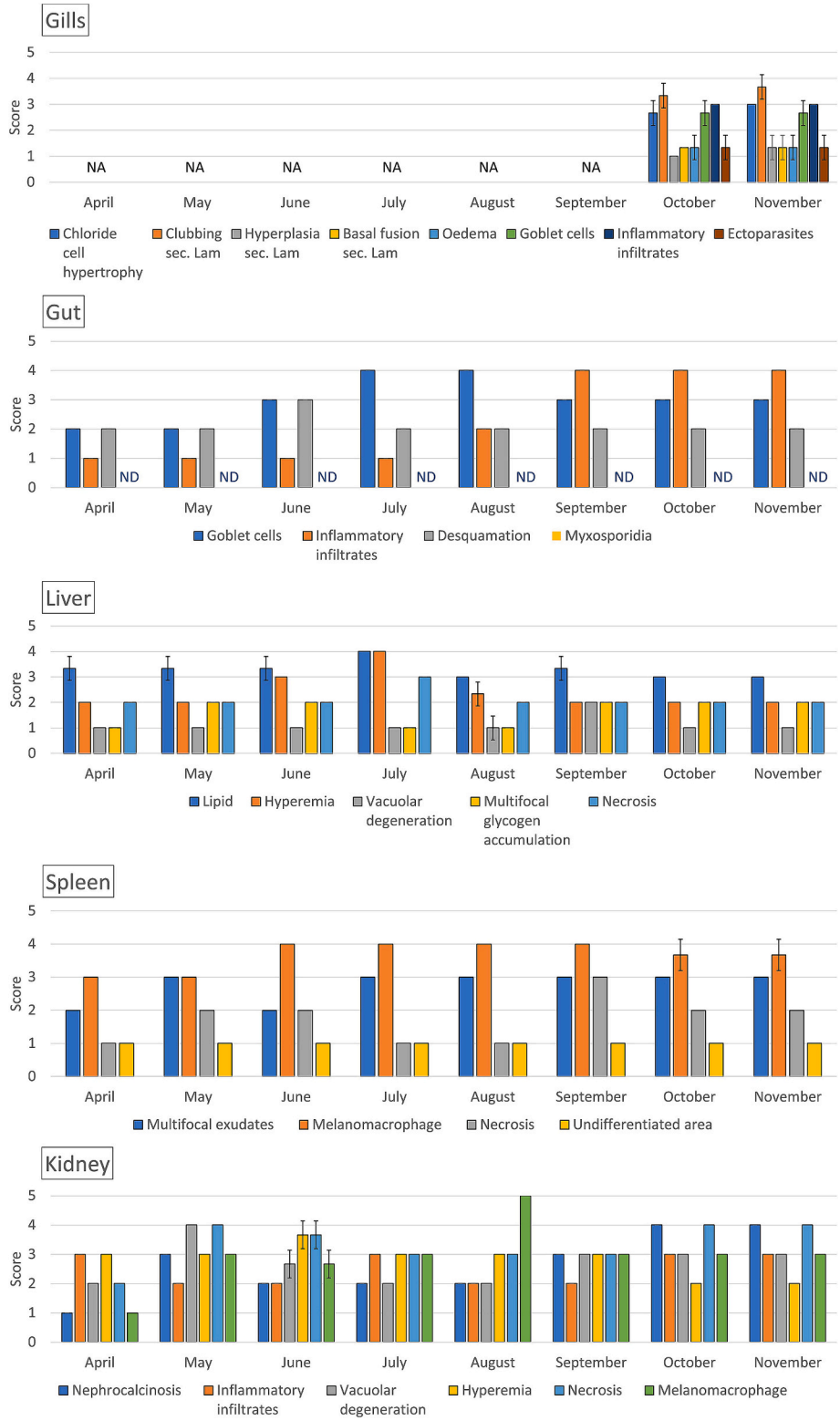

Fig. 9. Fish tissue histopathological scoring system mean scores (±SD) for each analyzed organ and histopathological parameter over monthly sampling timepoints ($n = 3$ per time points from April to November). NA Not Available; ND: Not detected.

(From April to November 2021) of the production cycle for *Seriola lalandi* in a commercial Recirculating Aquaculture System (RAS), examining key elements such as water quality, microbiota biodiversity and fish health.

4.1. The influence of water quality parameters on fish welfare

Given the high stocking density and the recirculating nature of RAS, maintaining optimal water quality is a crucial yet challenging aspect of the system's overall success. Several parameters were monitored in the present study including CO_2, water temperature, pH, nitrogen

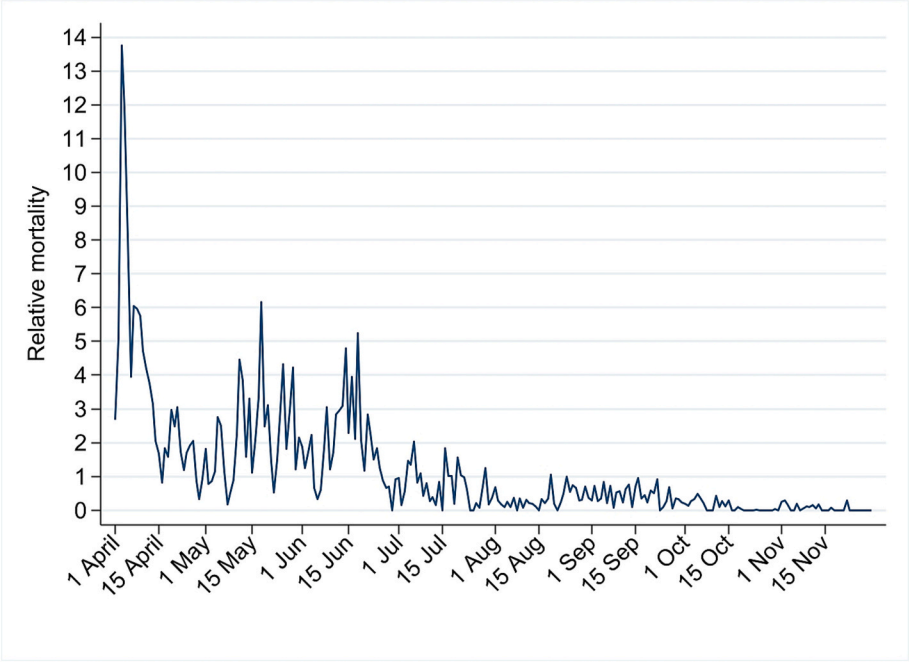

Fig. 10. The Relative fish mortality during the study period is denoted as the fold-change in dead fish biomass on any day in comparison to the dead biomass recorded on a randomly selected date (January 1st). This parameter was selected to ensure the confidentiality of sensitive farm data.

compounds and H_2S.

Limiting the buildup of respiratory CO_2 is essential in RAS (Summerfelt et al., 2000) as elevated values can adversely affect the physiology, behavior, and productivity of farmed fish (Pan et al., 2020). In this study, CO_2 concentration was consistently maintained below 10 mg/L, which is within the recommended concentration range for kingfish (Pan et al., 2020). For instance, juvenile *S. lalandi* (≈ 230 g) showed a concentration-dependent reduction of the mass-specific growth rate (SGR_m) from $[CO_2] \geq 19.38$ mg/L (Pan et al., 2020). This threshold is comparable to that of Atlantic salmon, which ranges between 10 and 20 mg/L $[CO_2]$ according to different studies (Fivelstad et al., 2003; Good et al., 2018; Khan et al., 2018). It is slightly higher than for Atlantic cod (*Gadus morhua*) which shows impairment from $[CO_2] \geq 8$ mg/L (Moran and Støttrup, 2011).

In the studied RAS, the mean water temperature ranged between 20 °C and 25 °C, peaking around June. The optimal water temperature for juvenile kingfish was determined to be 26.5 °C, resulting in a 54 % increase in weight after 30 days as compared to fish reared at 21 °C (Abbink et al., 2012). Also, pH plays a critical role in fish welfare. In the analyzed facility, careful pH management was implemented, initially setting it around 7.8 until July and later stabilizing it at 7.5. Previous studies showed that kingfish juveniles (≈32 g) maintained unaltered growth and feed conversion ratio (FCR) down to a pH of 7.16 when compared to the ambient pH of 7.85. However, at a lower pH of 6.58, mortality was observed, accompanied by inhibited growth and reduced FCR (Abbink et al., 2012). Both temperature and pH of the analyzed RAS fell within optimal ranges for *Seriola* growth.

Excessive accumulation of inorganic nitrogen compounds might result in reduced growth (Khan et al., 2018; Tomasso, 1994; Wajsbrot et al., 1993) immune depression (Gonçalves et al., 2012; Hurvitz and Bercovier, 1997; Li et al., 2013) and mortality (Lemarié et al., 2004; Meade, 1985; Russo and Thurston, 1991; Ruyet et al., 1995). Nitrogen compounds include ammonia [either ionized (NH_4^+) or un-ionized (NH_3)], nitrite (NO_2^-) and nitrate (NO_3^-). In the present study, NH_3 levels were below 0.01 mg/L, and NH_4^+ levels were below 0.6 mg/L. These concentrations fall within the recommended safety limits for various cultured species. For salmonids, NH_3 should not exceed 0.0125 mg/L (Timmons et al., 2018), while total ammonia nitrogen (TAN) for sea bass adults should be below 2 mg/L (Lemarié et al., 2004). The second nitrogen compound, nitrite (NO_2^-) is toxic for most farmed species (Ciji and Akhtar, 2020). In the present study, NO_2^- was <0.3 mg/L. This falls below the suggested safety limit of 0.75 mg/L NO_2^- for juvenile *S. lalandi* (Abbink et al., 2012) and 1.0 mg/L for juvenile Atlantic cod (*Gadus morhua*) (Siikavuopio and Sæther, 2006). Throughout most of the sampling period, the concentration of NO_3^- remained below 300 mg/L, with a brief increase reaching 450 mg/L for two weeks in August. Nitrate concentrations for large marine fish are recommended to be lower than 500 mg/L (Pierce et al., 1993). While nitrate is not as toxic as other nitrogen compounds, chronic exposure can impact fish growth and health. As an example, rainbow trout (*Onchorhynchus mykiss*) exposed to 80–100 mg/L NO_3^- for three months exhibited abnormal swimming behavior and mildly reduced survival (Davidson et al., 2014). Juvenile turbot (*Psetta maxima*) exposed to 124 mg/L NO_3^- for 6 weeks showed decreased specific growth rate (SGR) and biomass yield (van Bussel et al., 2012), while African catfish (*Clarias gariepinus*) experienced reduced growth and feed intake at 379 mg/L NO_3^- over 42 days (Schram et al., 2014). In contrast to rainbow trout, post-smolt Atlantic salmon showed no significant effects on growth and welfare when chronically exposed to 100 mg/L NO_3^- for 8 months (Davidson et al., 2017). To the best of the authors' knowledge, it is not known whether chronic exposure to nitrate could impair growth rates, appetite, or general welfare in *Seriola lalandi*. Indeed, no evident signs of impaired fish health were reported in this study.

H_2S represents a serious concern in RAS, leading to sudden mortality in several farmed fish species (Hjeltnes et al., 2019; Sommerset et al., 2020). In the present study, H_2S was consistently below 20 μg/L throughout the sampling timeframe. This value is well below the critical concentration for other saltwater fish species. For instance, physiological investigations in post-smolt Atlantic salmon revealed that H_2S disrupts metabolism by reducing oxygen uptake below the standard metabolic rate, starting at a concentration of 60.7 ± 13.3 μg/L (Bergstedt and Skov, 2023). Interestingly, Atlantic salmon exhibit changes in swimming behavior in response to the presence of H_2S, indicating signs of distress at concentrations well below the critical toxic threshold (Ciani et al., 2024a). The response to H_2S differs among species, likely depending on physiological adaptations to different habitats.

Critical concentrations that result in acute mortality span from LC_{50} 0.25 to 53 μM (Bagarinao and Vetter, 1989; Smith and Oseid, 1974). Indeed, since no signs of distress or increased mortality rates were observed in the kingfish within the analyzed RAS, it appears that this fish species is tolerating well the H_2S concentration (20 μg/L) measured over the sampling period.

4.2. The role of the predominant microorganisms in fish and RAS samples

The microbial community plays a crucial role in RAS, influencing both water quality and the overall health of the fish (Preena et al., 2021; Rurangwa and Verdegem, 2015). It's challenging to fully map the microbiota in RAS because it varies at all levels - not just between different systems, but also within sites of the same system, among fish in the same tank, and even between tissues of the same fish (Preena et al., 2021; Rurangwa and Verdegem, 2015). There is a gap in the literature when it comes to the comprehensive analysis of the microbiota composition of entire systems. In this study, 16S rRNA gene amplicon sequencing was utilized to examine the microbial structure across various sites and individual fish within the RAS. The analysis covered three fish tissues (skin, gills, and intestine) and multiple locations within the RAS, including tank water, tank wall biofilm, biofilter biofilm and denitrification unit. The sensitivity of 16S sequencing allowed the classification of bacteria primarily at the genus or family level, with only a few identified as species.

The most abundant genera in **RAS samples** were *Erythrobacter* (up to 57.0 %), *Glaciecola* (up to 41.0 %), and *Nitrospira* (up to 23.7 %). The genus *Erythrobacter*, known for its carotenoid production, is widely distributed in marine ecosystems (Yoon et al., 2022). Likewise, the genus *Glaciecola* is relatively abundant in marine environments and was identified in aquaculture sites at sea, where both seabream (*Sparus aurata*) and seabass (*Dicentrarchus labrax*) were cultivated (Kyritsi et al., 2023). Furthermore, *Glaciecola* has been recognized as a core member of the water microbiota in farmed rockfish (*Sebastes schlegelii*) (Jiang et al., 2020). Considering their substantial presence in marine environments, it is unsurprising to find them in high concentrations in the studied RAS. The *Nitrospira* genus includes nitrite-oxidizing bacteria (NOB) capable of oxidizing inorganic nitrogen compounds (Gruber, 2008; Mancinelli, 1996). This genus represented the most abundant group of NOB found in the denitrification unit of RAS farming in both marine (Ruan et al., 2015) and brackish water (Kruse et al., 2013) fish species. This was attributed to its higher substrate affinity (Urakawa et al., 2008) allowing it to utilize nitrite and oxygen more efficiently compared to other genera like *Nitrobacter* (Rurangwa and Verdegem, 2015).

The most abundant genera in fish samples were *Aliivibrio* (up to 79.8 %), *Pseudomonas* (up to 75.4 %), and an uncultured genus from the family *Mycoplasmataceae* (up to 73.1 %). The genus *Aliivibrio* includes five species (Beaz-Hidalgo et al., 2010), of which three have been associated with diseases in Atlantic salmon, namely *A. salmonicida* (Egidius et al., 1986), *A. wodanis* (Lunder et al., 2000) and *A. logei* (Benediktsdóttir et al., 1998). Despite the presence of this genus, no disease outbreaks were reported in this study. Possible explanations include the limited presence of pathogenic species, a robust immune system of the fish preventing outbreaks, a lower sensitivity of *S. lalandi* compared to salmon, or a combination of the above. On the other hand, the genus *Pseudomonas* has been recommended as a probiotic bacterium for application in aquaculture for its potential benefits to fish health (Balcázar et al., 2006; Gatesoupe, 1999, 2007; Irianto and Austin, 2002; Rurangwa and Verdegem, 2015) being part of the core gut microbiota of fish (Gioacchini et al., 2018). It has been also identified in playing a key role in breaking down Geosmin and 2-Methylisoborneol (MIB) (Hoefel et al., 2006; Izaguirre et al., 1988) and contributing to denitrification in RAS (Brown et al., 2013; Preena et al., 2021; Schreier et al., 2010). The family *Mycoplasmataceae* generally has a parasitic or saprophytic lifestyle, living in close association with their hosts to fulfill their nutritional requirements (Sellyei et al., 2021). Mycoplasmas are commonly detected in the gastrointestinal tract of fish (Brown et al., 2019; Holben et al., 2002). This family was a major component in the intestine of healthy fish from several species including striped bass (hybrid *Moron saxatilis* × *Moron chrysops*), European seabass (*Dicentrarchus labrax*) red drum (*Sciaenops ocellatus*); tilapia (hybrid *Oreochromis aureus x Oreochromis niloticus*) flathead grey mullet (*Mugil cephalus*) and the common carp (*Cyprinus carpio*) (Ofek et al., 2021). Previous research has proposed that the presence of Mycoplasmas in other organs might indicate pathological processes (Stadtländer and Kirchhoff, 1990). Contrary with what was previously indicated, *Mycoplasmataceae* were also identified in the gills, kidneys and liver of healthy fish in different carnivorous freshwater species, such as pike (*Esox Lucius*), wels catfish (*Silurus glanis*), black bullhead (*Ameiurus melas*) and pike perch (*Sander lucioperca*) (Sellyei et al., 2021). The high abundance of this taxa detected in the healthy fish analyzed in this study suggests that Mycoplasmas are commonly present in kingfish tissues under standard farming conditions.

4.3. Microbiota dynamics across different RAS sites and fish tissues

Indeed, focusing solely on the most abundant taxa would provide only partial information about the microbial structure of a system. In this study, cluster analyses were employed to identify distinctive biodiversity compositions among various samples, while NMDS analysis was utilized to observe any temporal shifts in microbial composition within each sample. Notably, two clusters were composed of tank water, gill, and skin mucus samples. This indicates a similar bacterial configuration between these fish tissues and the tank water, emphasizing their profound connection with the external environment. Furthermore, the microbiota composition in water, skin, and gills underwent monthly changes over time, particularly noticeable from April to July. Although these differences persisted, they became less pronounced from August onward. This shift in microbial communities reflects the fluctuations in water parameters, which exhibited variation from April to July but were then stabilized from August onward. These findings highlight the importance of microbial composition in skin and gill tissues as a highly relevant factor for fish health and welfare, given their strict connection with the surrounding environment. Including these tissues in future investigations could provide valuable insights into disease risk in RAS.

All other samples from the RAS were grouped into a single cluster, suggesting minimal variation in microbiota between the tank biofilm, biofilter biofilm and denitrification unit. According to NMDS analysis, the tank wall biofilm and biofilter biofilm were stable over time suggesting that they are less susceptible to changes in water parameters. In contrast, the denitrification unit displayed temporal fluctuations in the microbial community. Water parameters, including temperature, pH, salinity, dissolved oxygen, and substrate concentration, play crucial roles in influencing the composition of the nitrifying community in RAS (Bakke et al., 2017; Rangaswamy et al., 2020). Within the denitrification unit, pH ranged from 5.3 to 6.1 from April to June, stabilized around 7 from July to October, and then rose again in November to approximately 8.3. Simultaneously, the temperature fluctuated over time, with mean temperatures around 18–19 °C in April, May, and December, and higher temperatures between June and October. These variations could have contributed to the observed shifts in the microbial composition of the denitrification unit.

The remaining tissue samples were organized into six clusters. Among these, four included a combination of skin, intestine, and gill samples, highlighting a shared microbiota composition across various tissues. Notably, the intestine samples exhibited two distinct clusters, indicating a possible variation in the microbial composition throughout different phases of the production cycle. Substantiating this, NMDS analysis confirmed the temporal changes in intestine samples, with more pronounced monthly variations observed from April to July, while differences between August and November were comparatively lower. This variability could be associated with differences in the individual fish's

physiological status, age, or size, as well as being influenced by changes in water parameters.

Microbial community dynamics in RAS environments, in particular in tank water and tank biofilms, show significant correlations with the hosted fish, mediated by both environmental and physiological variations (Dahle et al., 2023). An r/K-selection model hypothesis suggested that K-selection strategies result in different water microbiota with fewer opportunistic bacteria, which in turn influence the microbiota of fish larvae (Vadstein et al., 2018). Similarly, Nile tilapia larvae cultured in two different production systems (biofloc and flow-through) exhibited variation in growth performance and gut microbiomes (Deng et al., 2022). However, to what extent these microbiota dynamics are attributed to environmental or physiological changes remains unclear.

4.4. Occurrence of three selected pathogens in RAS and fish samples

While amplicon sequencing of the 16S gene provides valuable insights into the microbial diversity and composition, it may not be the most suitable tool for detecting potential pathogens due to its low sensitivity at the species level and long processing times. To address this limitation, specific digital PCR (dPCR) assays were developed for the absolute quantification of three known fish pathogens [*Vibrio harveyi* (Makridis et al., 2021; Zhang et al., 2020), *Vibrio anguillarum* (Castillo et al., 2015; Frans et al., 2011), and *Photobacterium damselae* (Romalde, 2002)] throughout the analyzed timeframe. The dPCR assay demonstrated the capability to detect even a few copies of target DNA in the sampled RAS sites and fish, making it a valuable tool for high-resolution pathogen monitoring. Generally, the targeted species were either present at very low levels (<20 copies/ng-DNA) or completely absent from most of the samples. Of particular interest for fish health, the DNA of all three species was present at low levels in the tank water samples, with the highest concentrations detected in August and September. However, it is not possible to directly correlate the amount of DNA detected with the exact number of virulent cells and the concentrations measured were below the threshold at which a fish would show any signs of vibriosis or pasteurellosis. In summary, the results demonstrated the sensitivity of the applied dPCR approach to detect the presence of potential pathogens in different sample types and also at very low pathogen occurrences.

4.5. Histopathological observations and their connection with fish health

Histopathological analysis revealed the occurrence of almost all parameters investigated in the different fish tissues. It is important to emphasize that most of the factors examined in this study are not inherently negative when occurring at low levels and can be naturally present in overall healthy fish (Wolf, 2018; Wolf et al., 2015). However, an increase in their occurrence may serve as an indicator of compromised fish health conditions.

An increase in inflammatory cells was detected in the intestine from August onward. Pathogens can enter through the oral cavity when water or food is contaminated (Weber et al., 2010) and impact the intestine (Frans et al., 2011). This could cause inflammation despite the intestine's natural defenses, including acidity, bile salts, enzymes, and mucus secreted by goblet cells (Frans et al., 2011; Magnadóttir, 2006). While the observed increase in inflammation coincided with the period during which the three pathogens (*P. damselae, V. harveyi* and *V. anguillarum*) were detected in the tank water, *V. anguillarum* was found in the intestine only in December, whereas the others were never detected. It is reasonable to suggest that the fish's immune system effectively limited the proliferation of pathogens, resulting in both the observed increase in inflammation and the absence of detectable bacteria in the tissue. One could also speculate that the presence of these pathogen in the water might be associated with the presence of other, uninvestigated, pathogens. While both hypotheses remain to be validated, it is important to consider that inflammation is a non-specific physiological response triggered by a wide array of stressors beyond pathogens (Campos-Sánchez and Esteban, 2021). Interestingly, the study also revealed a peak in intestinal desquamation in June. The process of desquamation, characterized by the shedding of living cells from the epithelium, may reduce absorption capacity by diminishing the area available for digestion to take place (Polistovskaya et al., 2018). Causes of intestinal epithelial desquamation often involve parasites, pathogens, and exposure to heavy metals like zinc, cadmium, and copper (Sitjà-Bobadilla et al., 2016). However, in the current study, no parasites were identified in the intestine and water quality parameters were generally good and within safety limits suggested in the bibliography, as previously discussed.

Following initial infection, pathogens can spread to other organs, including the liver, spleen, and kidney, via the bloodstream (Frans et al., 2011). In June, there was an increase in desquamation in the intestine and melanomacrophage centers in the spleen. This was followed by increased hyperemia, lipid accumulation and necrosis in the liver in July, and an increase in melanomacrophage centers in the kidneys in August. Recent research indicates that *Vibrio* pathogens can impact liver hyperemia and fat accumulation, both of which may lead to organ necrosis (Duman et al., 2022) while *P. damselae* induces an increase in melanomacrophage centers in both the kidney and spleen (Eissa et al., 2018; El-Son et al., 2020; Essam et al., 2016; Manrique et al., 2014). Nonetheless, as already described, the fish didn't develop vibriosis or pasteurellosis. This might be indicative of the low presence of the bacteria, the proper functioning of the fish's immune system, or a combination of those factors. Besides spleen melanomacrophages, which remained high until the end of the study period, all other parameters decreased after the peak.

Gill samples were collected exclusively during October and November. Within this period, a moderate hypertrophy of chloride cells, along with the presence of inflammatory cells and clubbing of secondary lamellae, was noted. Several causes might have induced such factors. Exposure to heavy metals, high ammonia levels, low pH, parasites, or pathogens can induce hypertrophy of chloride cells, inflammation, or clubbing of secondary lamellae (Strzyzewska et al., 2016; Zawisza et al., 2024). Clubbing often coincides with the presence of gill parasites as demonstrated in both marine [Atlantic salmon (*Salmo solar*) (Clark et al., 1997)] and freshwater [Rohu (*Labeo rohita*) and Mrigal carp (*Cirrhinus mrigala*) (Ahmed et al., 1998)] species. Ectoparasites were observed via histology during the study period, albeit at very low levels. The presence of ectoparasites, coupled with the bacterial pathogen in the water, could be some of the factors contributing to the observed hyperplasia of chloride cells and the moderate inflammation detected.

Considering environmental factors, microbiology data, and the overall conditions of the rearing environment can enhance the quality of the information obtained from histopathological evaluations alone. Adopting this holistic approach ensures a comprehensive understanding of the observed indices and their implications for fish health. One limitation of this particular study may result from the relatively low number of biological replicates per timepoint, as three fish may not adequately represent the health status of the entire batch within a tank. However, it is noteworthy that the variation between replicates was minimal, with most fish displaying similar values for each parameter at any given timepoint. Despite this limitation, the development of a histological protocol for analyzing various tissues in *Seriola lalandi* serves as a valuable tool for assessing the health status of this species throughout a production cycle.

4.6. Mortality rates

Mortality rates, measured as biomass loss, showed a decline starting in June. When considering these rates in terms of the number of dead fish, the decline would become even more pronounced. This is because, with fish growth over time, an equivalent biomass loss later in the production cycle corresponds to fewer fish compared to earlier stages. The reduction in mortality rates may be attributed to several factors.

First, weaker fish might have succumbed earlier, leaving behind a hardier population. Additionally, both changes in water parameters and shifts in the microbial community could have contributed to the observed decrease.

The water temperature increased from 22 °C to 24 °C in June. Juvenile kingfish exhibit enhanced growth when water temperature is raised from 21 °C to 26 °C. The temperature increase in this study brought conditions closer to the optimal range for juvenile fish (Abbink et al., 2012). Salinity, which initially fluctuated around 24 ppt (or g/L), was gradually reduced and stabilized at 19 ppt. Compared to seawater salinity (35 ppt), rearing kingfish in brackish water (17 ppt) has been shown to improve growth by reducing osmoregulatory costs, which lowers resting cardiorespiratory activity and results in energetic savings (Morgenroth et al., 2022). Oxygen saturation exceeded 100 %, peaking at 150 % at the end of May. From June onward, it stabilized at approximately 110 % to mitigate the risks associated with oxygen supersaturation and total gas pressure. Hyperoxia can impact fish physiology, inducing hypoventilation and leading to carbon dioxide retention, which may cause respiratory acidosis (McArley et al., 2021). A shift in the microbial community was observed over the sampling period in both the RAS and fish samples, concomitant with changes in water parameters. Previous studies have indicated that such changes in microbial communities can impact fish physiology (Dahle et al., 2023; Deng et al., 2022; Vadstein et al., 2018).

Together, the increase in temperature and reductions in pH, salinity, and oxygen saturation—bringing these parameters closer to optimal levels—along with shifts in the microbial community, may have alleviated physiological stress in the fish and contributed to reduced mortality rates.

5. Conclusion

This study presents a comprehensive analysis of a *Seriola lalandi* production cycle within a commercial RAS. It produced an extensive dataset of the microbiota composition of both fish tissues (skin, gills and intestine) and RAS components (biofilter, tank water, denitrification unit). Additionally, it introduced a Multiparametric Semi-quantitative Scoring System (MSSS) for histological assessment of the gills, intestine, liver, spleen and kidney. While the study was not designed to establish causality, it revealed interdependencies among various observed parameters, particularly the reduction in mortality following the optimization of water parameters and a shift in microbial communities, suggesting that refining system management and monitoring techniques could enhance the sustainability and productivity of aquaculture operations.

Supplementary data to this article can be found online at https://doi.org/10.1016/j.aquaculture.2025.742851.

Ethical statement for experimental animals

The experiment was performed according to EU regulations concerning the protection of experimental animals (Directive 2010/63/EU). Appropriate measures were taken to minimize pain and discomfort.

CRediT authorship contribution statement

Katerina Loufi: Writing – review & editing, Visualization, Methodology, Formal analysis, Data curation. **Julia Hassa:** Writing – review & editing, Visualization, Methodology, Formal analysis, Data curation. **Eric Hernández:** Writing – review & editing, Resources, Investigation, Data curation. **Marit Stormoen:** Writing – review & editing, Resources. **Deni Ribičić:** Writing – review & editing, Project administration, Conceptualization. **Stamatios Kapasakis:** Methodology, Data curation. **Tobias Busche:** Writing – review & editing, Resources. **Jörn Kalinowski:** Writing – review & editing, Resources. **Pavlos Makridis:** Writing – review & editing, Resources, Investigation, Conceptualization. **Roman Netzer:** Writing – review & editing, Resources, Project administration, Methodology, Conceptualization. **Elia Ciani:** Writing – review & editing, Writing – original draft, Visualization, Project administration, Methodology, Formal analysis, Data curation, Conceptualization.

Funding

The study was financed from the ERA-NET Cofund on Blue Bioeconomy (BlueBio) program as part of the DigiRAS project (Project number 311891).

Declaration of competing interest

The authors declare the following financial interests/personal relationships which may be considered as potential competing interests:

Eric Hernandez reports a relationship with InfiniteSea GmbH that includes: employment. If there are other authors, they declare that they have no known competing financial interests or personal relationships that could have appeared to influence the work reported in this paper.

Acknowledgements

The authors are grateful to InfiniteSea GmbH staff for the professional conduction of the experiment and collection of the scientific material.

Data availability

Data will be available on request.

References

Abbink, W., Blanco Garcia, A., Roques, J.A.C., Partridge, G.J., Kloet, K., Schneider, O., 2012. The effect of temperature and pH on the growth and physiological response of juvenile yellowtail kingfish *Seriola lalandi* in recirculating aquaculture systems. Aquaculture 330–333, 130–135. https://doi.org/10.1016/j.aquaculture.2011.11.043.

Ahmed, N., Turchini, G.M., 2021. Recirculating aquaculture systems (RAS): environmental solution and climate change adaptation. J. Clean. Prod. 297, 126604. https://doi.org/10.1016/j.jclepro.2021.126604.

Ahmed, G.U., Haque, M.M., Hoque, M.J., 1998. Gill pathology of juvenile carps in nursery pond. Bangladesh J. Fish Res. 2, 63–67.

Alipio, H.R.D., Bergstedt, J.H., Lazado, C.C., 2023. Differential sensitivity of mucosal organs to transient exposure to hydrogen sulphide in post-smolt Atlantic salmon (*Salmo salar*). Aquaculture 573, 739595. https://doi.org/10.1016/j.aquaculture.2023.739595.

Andrews, S., 2010. FastQC: A Quality Control Tool for High Throughput Sequence Data. No Title.

Badiola, M., Mendiola, D., Bostock, J., 2012. Recirculating aquaculture systems (RAS) analysis: main issues on management and future challenges. Aquac. Eng. 51, 26–35. https://doi.org/10.1016/j.aquaeng.2012.07.004.

Bagarinao, T., Vetter, R.D., 1989. Sulfide tolerance and detoxification in shallow-water marine fishes. Mar. Biol. 103, 291–302. https://doi.org/10.1007/BF00397262.

Bakke, I., Åm, A.L., Kolarevic, J., Ytrestøyl, T., Vadstein, O., Attramadal, K.J.K., Terjesen, B.F., 2017. Microbial community dynamics in semi-commercial RAS for production of Atlantic salmon post-smolts at different salinities. Aquac. Eng. 78, 42–49. https://doi.org/10.1016/j.aquaeng.2016.10.002.

Balcázar, J.L., de Blas, I., Ruiz-Zarzuela, I., Cunningham, D., Vendrell, D., Múzquiz, J.L., 2006. The role of probiotics in aquaculture. Vet. Microbiol. 114, 173–186. https://doi.org/10.1016/j.vetmic.2006.01.009.

Beaz-Hidalgo, R., Doce, A., Balboa, S., Barja, J.L., Romalde, J.L., 2010. *Aliivibrio finisterrensis sp.* nov., isolated from Manila clam, *Ruditapes philippinarum* and emended description of the genus *Aliivibrio*. Int. J. Syst. Evol. Microbiol. 60, 223–228. https://doi.org/10.1099/ijs.0.010710-0.

Benediktsdóttir, E., Helgason, S., Sigurjónsdóttir, H., 1998. Vibrio spp. isolated from salmonids with shallow skin lesions and reared at low temperature. J. Fish Dis. 21, 19–28. https://doi.org/10.1046/J.1365-2761.1998.00065.X.

Bergstedt, J.H., Skov, P.V., 2023. Acute hydrogen sulfide exposure in post-smolt Atlantic salmon (*Salmo salar*): critical levels and recovery. Aquaculture 570, 739405. https://doi.org/10.1016/j.aquaculture.2023.739405.

Bernet, D., Schmidt, H., Meier, W., Burkhardt-Holm, P., Wahli, T., 1999. Histopathology in fish: proposal for a protocol to assess aquatic pollution. J. Fish Dis. 22, 25–34. https://doi.org/10.1046/J.1365-2761.1999.00134.X.

Bokulich, N.A., Kaehler, B.D., Rideout, J.R., Dillon, M., Bolyen, E., Knight, R., Huttley, G. A., Gregory Caporaso, J., 2018. Optimizing taxonomic classification of marker-gene

amplicon sequences with QIIME 2's q2-feature-classifier plugin. Microbiome 6, 90. https://doi.org/10.1186/s40168-018-0470-z.
Bolyen, E., Rideout, J.R., Dillon, M.R., Bokulich, N.A., Abnet, C.C., Al-Ghalith, G.A., Alexander, H., Alm, E.J., Arumugam, M., Asnicar, F., 2019. Reproducible, interactive, scalable and extensible microbiome data science using QIIME 2. Nat. Biotechnol. 37, 852–857.
Brown, M.N., Briones, A., Diana, J., Raskin, L., 2013. Ammonia-oxidizing archaea and nitrite-oxidizing nitrospiras in the biofilter of a shrimp recirculating aquaculture system. FEMS Microbiol. Ecol. 83, 17–25. https://doi.org/10.1111/j.1574-6941.2012.01448.x.
Brown, R.M., Wiens, G.D., Salinas, I., 2019. Analysis of the gut and gill microbiome of resistant and susceptible lines of rainbow trout (*Oncorhynchus mykiss*). Fish Shellfish Immunol. 86, 497–506.
Callahan, B.J., McMurdie, P.J., Rosen, M.J., Han, A.W., Johnson, A.J.A., Holmes, S.P., 2016. DADA2: high-resolution sample inference from Illumina amplicon data. Nat. Methods 13, 581–583.
Campos-Sánchez, J.C., Esteban, M.Á., 2021. Review of inflammation in fish and value of the zebrafish model. J. Fish Dis. 44, 123–139. https://doi.org/10.1111/jfd.13310.
Castillo, D., D'Alvise, P., Middelboe, M., Gram, L., Liu, S., Kalatzis, P.G., Kokkari, C., Katharios, P., 2015. Draft genome sequences of the fish pathogen Vibrio harveyi strains VH2 and VH5. Genome Announc. 3. https://doi.org/10.1128/genomeA.01062-15 e01062–15.
Ciani, E., Kvæstad, B., Stormoen, M., Mayer, I., Gupta, S., Ribičić, D., Netzer, R., 2024a. Early warning through video monitoring: dissolved hydrogen sulphide (H2S) affects Atlantic salmon swimming behavior in recirculating aquaculture systems. Aquaculture 581. https://doi.org/10.1016/j.aquaculture.2023.740201.
Ciani, E., Lie, K.-I., Stormoen, M., Antonsen, S.I., Jørgensen, E.H., 2024b. Histopathological assessment of Atlantic salmon exposed to calcium oxide particles: a controlled clinical study. Front. Aquac. 2. https://doi.org/10.3389/faquc.2023.1307835.
Ciji, A., Akhtar, M.S., 2020. Nitrite implications and its management strategies in aquaculture: a review. Rev. Aquac. 12, 878–908. https://doi.org/10.1111/raq.12354.
Clark, A., Nowak, B., Handlinger, J., Munday, B.L., Percival, S., 1997. Clubbing and necrosis gill (CNG) syndrome in sea-caged Atlantic salmon, *Salmo salar* L., in Tasmania: an initial report. J. Fish Dis. 20, 59–68. https://doi.org/10.1046/j.1365-2761.1997.d01-109.x.
Dahle, S.W., Gaarden, S.I., Buhaug, J.F., Netzer, R., Attramadal, K.J.K., Busche, T., Aas, M., Ribicic, D., Bakke, I., 2023. Long-term microbial community structures and dynamics in a commercial RAS during seven production batches of Atlantic salmon fry (*Salmo salar*). Aquaculture 565, 739155. https://doi.org/10.1016/j.aquaculture.2022.739155.
Dalsgaard, J., Lund, I., Thorarinsdottir, R., Drengstig, A., Arvonen, K., Pedersen, P.B., 2013. Farming different species in RAS in Nordic countries: current status and future perspectives. Aquac. Eng. 53, 2–13.
Davidson, J., Good, C., Welsh, C., Summerfelt, S.T., 2014. Comparing the effects of high vs. low nitrate on the health, performance, and welfare of juvenile rainbow trout Oncorhynchus mykiss within water recirculating aquaculture systems. Aquac. Eng. 59, 30–40.
Davidson, J., Good, C., Williams, C., Summerfelt, S.T., 2017. Evaluating the chronic effects of nitrate on the health and performance of post-smolt Atlantic salmon *Salmo salar* in freshwater recirculation aquaculture systems. Aquac. Eng. 79, 1–8. https://doi.org/10.1016/j.aquaeng.2017.08.003.
Deng, Y., Verdegem, M.C.J., Eding, E., Kokou, F., 2022. Effect of rearing systems and dietary probiotic supplementation on the growth and gut microbiota of Nile tilapia (*Oreochromis niloticus*) larvae. Aquaculture 546, 737297. https://doi.org/10.1016/j.aquaculture.2021.737297.
Drønen, K., Roalkvam, I., Nilsen, H., Olsen, A.B., Dahle, H., Wergeland, H., 2022. Presence and habitats of bacterial fish pathogen relatives in a marine salmon post-smolt RAS. Aquac. Rep. 26, 101312.
Duman, M., Altun, S., Ozdemır, B., Satıcıoglu, I.B., 2022. Fatty liver disease and bacterial co-infection in cultured marine fish. Erciyes Üniversitesi Vet. Fakültesi Derg. 19, 1–10.
Egidius, E., Wiik, R., Andersen, K., Hoff, K.A., Hjeltnes, B., 1986. Vibrio salmonicida sp. nov., a new fish pathogen. Int. J. Syst. Bacteriol. 36, 518–520. https://doi.org/10.1099/00207713-36-4-518.
Eissa, I.A.M., Derwa, H.I., Ismail, M., El-Lamie, M., Dessouki, A.A., Elsheshtawy, H., Bayoumy, E.M., 2018. Molecular and phenotypic characterization of Photobacterium damselae among some marine fishes in Lake Temsah. Microb. Pathog. 114, 315–322.
El-Son, M.A.M., Elbahnaswy, S., Ibrahim, I., 2020. Molecular and histopathological characterization of Photobacterium damselae in naturally and experimentally infected Nile tilapia (*Oreochromis niloticus*). J. Fish Dis. 43, 1505–1517. https://doi.org/10.1111/jfd.13251.
Essam, H.M., Abdellrazeq, G.S., Tayel, S.I., Torky, H.A., Fadel, A.H., 2016. Pathogenesis of Photobacterium damselae subspecies infections in sea bass and sea bream. Microb. Pathog. 99, 41–50.
EUMOFA, 2020. Recirculation Aquaculture Systems. Publications Office of the European Union.
Fivelstad, S., Olsen, A.B., Åsgård, T., Baeverfjord, G., Rasmussen, T., Vindheim, T., Stefansson, S., 2003. Long-term sublethal effects of carbon dioxide on Atlantic salmon smolts (*Salmo salar* L.): ion regulation, haematology, element composition, nephrocalcinosis and growth parameters. Aquaculture 215, 301–319.
Fowler, A.J., Ham, J.M., Jennings, P.R., 2003. Discriminating between cultured and wild yellowtail kingfish (*Seriola lalandi*) in South Australia. Rep. PIRSA Aquac. SARDI Aquat. Sci. Publ. No RD030159 https://scholar.google.com/scholar?cites=15391535757452503554&as_sdt=2005&sciodt=0,5&hl=en.
Frans, I., Michiels, C.W., Bossier, P., Willems, K.A., Lievens, B., Rediers, H., 2011. *Vibrio anguillarum* as a fish pathogen: virulence factors, diagnosis and prevention. J. Fish Dis. 34, 643–661. https://doi.org/10.1111/j.1365-2761.2011.01279.x.
Fukui, Y., Sawabe, T., 2008. Rapid detection of Vibrio harveyi in seawater by real-time PCR. Microbes Environ. 23, 172–176.
Gatesoupe, F.J., 1999. The use of probiotics in aquaculture. Aquaculture 180, 147–165.
Gatesoupe, F.J., 2007. Live yeasts in the gut: natural occurrence, dietary introduction, and their effects on fish health and development. Aquaculture 267, 20–30.
Gioacchini, G., Ciani, E., Pessina, A., Cecchini, C., Silvi, S., Rodiles, A., Merrifield, D.L., Olivotto, I., Carnevali, O., 2018. Correction to: effects of Lactogen 13, a new probiotic preparation, on gut microbiota and endocrine signals controlling growth and appetite of Oreochromis niloticus juveniles. Microb. Ecol. 1. https://doi.org/10.1007/s00248-018-1194-0.
Gonçalves, A.F., Páscoa, I., Neves, J.V., Coimbra, J., Vijayan, M.M., Rodrigues, P., Wilson, J.M., 2012. The inhibitory effect of environmental ammonia on Danio rerio LPS induced acute phase response. Dev. Comp. Immunol. 36, 279–288.
Good, C., Davidson, J., Terjesen, B.F., Takle, H., Kolarevic, J., Bæverfjord, G., Summerfelt, S., 2018. The effects of long-term 20 mg/L carbon dioxide exposure on the health and performance of Atlantic salmon Salmo salar post-smolts in water recirculation aquaculture systems. Aquac. Eng. 81, 1–9.
Gruber, N., 2008. The marine nitrogen cycle: overview and challenges. Nitrogen Mar. Environ. 2, 1–50.
Hjeltnes, B., Bang-Jensen, B., Bornø, G., Haukaas, A., Walde, C.S., 2019. The Health Situation in Norwegian Aquaculture 2018 [WWW Document]. Nor. Vet. Inst. URL. https://www.google.com/search?sxsrf=AJOqlzXxPWq0urIL9NTEA0ZeSdsio5T6qw:1678794874825&q=hjeltnes+2019+The+health+situation+in+Norwegian+aquaculture&spell=1&sa=X&ved=2ahUKEwiGjqihrtv9AhULcvEDHd03C9wQBSgAegQICBAB&biw=918&bih=683&dpr=1.25 (accessed 3.14.23).
Hoefel, D., Ho, L., Aunkofer, W., Monis, P.T., Keegan, A., Newcombe, G., Saint, C.P., 2006. Cooperative biodegradation of geosmin by a consortium comprising three gram-negative bacteria isolated from the biofilm of a sand filter column. Lett. Appl. Microbiol. 43, 417–423. https://doi.org/10.1111/j.1472-765X.2006.01974.x.
Holben, W.E., Williams, P., Saarinen, M., Särkilahti, L.K., Apajalahti, J.H.A., 2002. Phylogenetic analysis of intestinal microflora indicates a novel Mycoplasma phylotype in farmed and wild Salmon. Microb. Ecol. 44, 175–185. https://doi.org/10.1007/s00248-002-1011-6.
Hurvitz, A., Bercovier, H., Van rijn, J., 1997. Effect of ammonia on the survival and the immune response of rainbow trout (*Oncorhynchus mykiss*, Walbaum) vaccinated againstStreptococcus iniae. Fish Shellfish Immunol. 7, 45–53. https://doi.org/10.1006/fsim.1996.0062.
Irianto, A., Austin, B., 2002. Probiotics in aquaculture. J. Fish Dis. 25, 633–642. https://doi.org/10.1046/j.1365-2761.2002.00422.x.
Izaguirre, G., Wolfe, R.L., Means, E.G., 1988. Degradation of 2-methylisoborneol by aquatic bacteria. Appl. Environ. Microbiol. 54, 2424–2431. https://doi.org/10.1128/aem.54.10.2424-2431.1988.
Jiang, Y., Liu, X., Xu, Y., Shi, B., Wang, B., 2020. Microbiota characteristics in Sebastes schlegelii intestine in early life stages. J. Oceanol. Limnol. 38, 275–287. https://doi.org/10.1007/s00343-019-9011-2.
Joshi, N.A., Fass, J.N., 2011. Sickle: A Sliding-Window, Adaptive, Quality-Based Trimming Tool for FastQ Files.
Katoh, K., Misawa, K., Kuma, K., Miyata, T., 2002. MAFFT: a novel method for rapid multiple sequence alignment based on fast Fourier transform. Nucleic Acids Res. 30, 3059–3066. https://doi.org/10.1093/nar/gkf436.
Khan, J.R., Johansen, D., Skov, P.V., 2018. The effects of acute and long-term exposure to CO2 on the respiratory physiology and production performance of Atlantic salmon (*Salmo salar*) in freshwater. Aquaculture 491, 20–27. https://doi.org/10.1016/j.aquaculture.2018.03.010.
Kiemer, M.C.B., Black, K.D., Lussot, D., Bullock, A.M., Ezzi, I., 1995. The effects of chronic and acute exposure to hydrogen sulphide on Atlantic salmon (*Salmo salar* L.). Aquaculture 135, 311–327. https://doi.org/10.1016/0044-8486(95)01025-4.
Kruse, M., Keuter, S., Bakker, E., Spieck, E., Eggers, T., Lipski, A., 2013. Relevance and diversity of nitrospira populations in biofilters of brackish RAS. PLoS One 8, e64737. https://doi.org/10.1371/journal.pone.0064737.
Kyritsi, M., Tsoureki, A., Koukaras, K., Kamidis, N., Krey, G., Michailidou, S., Argiriou, A., 2023. Seasonal dynamics of marine bacterial communities in aquaculture farms: the case of the northern Ionian coastal ecosystem (Mediterranean Sea). J. Mar. Sci. Eng. 11, 1332. https://doi.org/10.3390/jmse11071332.
Lemarié, G., Dosdat, A., Covès, D., Dutto, G., Gasset, E., Person-Le Ruyet, J., 2004. Effect of chronic ammonia exposure on growth of European seabass (*Dicentrarchus labrax*) juveniles. Aquaculture 229, 479–491. https://doi.org/10.1016/S0044-8486(03)00392-2.
Li, M., Chen, L., Qin, J.G., Li, E., Yu, N., Du, Z., 2013. Growth performance, antioxidant status and immune response in darkbarbel catfish *Pelteobagrus vachelli* fed different PUFA/vitamin E dietary levels and exposed to high or low ammonia. Aquaculture 406–407, 18–27. https://doi.org/10.1016/j.aquaculture.2013.04.028.
Llewellyn, M.S., Boutin, S., Hoseinifar, S.H., Derome, N., 2014. Teleost microbiomes: the state of the art in their characterization, manipulation and importance in aquaculture and fisheries. Front. Microbiol. 5. https://doi.org/10.3389/fmicb.2014.00207.
Lunder, T., Sørum, H., Holstad, G., Steigerwalt, A.G., Mowinckel, P., Brenner, D.J., 2000. Phenotypic and genotypic characterization of Vibrio viscosus sp. nov. and Vibrio wodanis sp. nov. isolated from Atlantic salmon (*Salmo salar*) with "winter ulcer". Int. J. Syst. Evol. Microbiol. 50, 427–450. https://doi.org/10.1099/00207713-50-2-427.

Magnadóttir, B., 2006. Innate immunity of fish (overview). Fish Shellfish Immunol. 20, 137–151. https://doi.org/10.1016/j.fsi.2004.09.006. Reviews in Fish Immunology.
Magoč, T., Salzberg, S.L., 2011. FLASH: fast length adjustment of short reads to improve genome assemblies. FLASH fast length adjust. Short Reads Improve Genome Assem. 27, 2957–2963.
Makridis, P., Kokou, F., Bournakas, C., Papandroulakis, N., Sarropoulou, E., 2021. Isolation of Phaeobacter sp. from larvae of Atlantic Bonito (*Sarda sarda*) in a Mesocosmos unit, and its use for the rearing of European seabass larvae (*Dicentrarchus labrax* L.). Microorganisms 9, 128. https://doi.org/10.3390/microorganisms9010128.
Mancinelli, R.L., 1996. the nature of nitrogen: an overview. Life Support Biosphere Sci. 3, 17–24.
Manrique, W.G., da Silva Claudiano, G., Petrillo, T.R., de Castro, M.P., Pereira Figueiredo, M.A., de Andrade Belo, M.A., de Moraes, J.R.E., de Moraes, F.R., 2014. Response of splenic melanomacrophage centers of *Oreochromis niloticus* (Linnaeus, 1758) to inflammatory stimuli by BCG and foreign bodies. J. Appl. Ichthyol. 30, 1001–1006. https://doi.org/10.1111/jai.12445.
Martin, M., 2011. Cutadapt removes adapter sequences from high-throughput sequencing reads. EMBnet. J. 17, 10–12. https://doi.org/10.14806/ej.17.1.200.
McArley, T.J., Sandblom, E., Herbert, N.A., 2021. Fish and hyperoxia—from cardiorespiratory and biochemical adjustments to aquaculture and ecophysiology implications. Fish Fish. 22, 324–355. https://doi.org/10.1111/faf.12522.
Meade, J.W., 1985. Allowable Ammonia for fish culture. Progress. Fish-Cult. 47, 135–145. https://doi.org/10.1577/1548-8640(1985)47<135:AAFFC>2.0.CO;2.
Moran, D., Støttrup, J.G., 2011. The effect of carbon dioxide on growth of juvenile Atlantic cod *Gadus morhua* L. Aquat. Toxicol. 102, 24–30. https://doi.org/10.1016/j.aquatox.2010.12.014.
Morgenroth, D., McArley, T., Danielo, Q., Harford, A., Hickey, A.J.R., Khan, J., Sandblom, E., 2022. Kingfish (*Seriola lalandi*) adjust to low salinity with only subtle effects to cardiorespiratory and growth performance. Aquaculture 556, 738268. https://doi.org/10.1016/j.aquaculture.2022.738268.
Netzer, R., Ribičić, D., Aas, M., Cavé, L., Dhawan, T., 2021. Absolute quantification of priority bacteria in aquaculture using digital PCR. J. Microbiol. Methods 183, 106171. https://doi.org/10.1016/j.mimet.2021.106171.
Ofek, T., Lalzar, M., Laviad-Shitrit, S., Izhaki, I., Halpern, M., 2021. Comparative study of intestinal microbiota composition of six edible fish species. Front. Microbiol. 12. https://doi.org/10.3389/fmicb.2021.760266.
Orellana, J., Waller, U., Wecker, B., 2014. Culture of yellowtail kingfish (*Seriola lalandi*) in a marine recirculating aquaculture system (RAS) with artificial seawater. Aquac. Eng. 58, 20–28. https://doi.org/10.1016/j.aquaeng.2013.09.004.
Østevik, L., Stormoen, M., Nødtvedt, A., Alarcón, M., Lie, K.-I., Skagøy, A., Rodger, H., 2021. Assessment of acute effects of *in situ* net cleaning on gill health of farmed Atlantic salmon (*Salmo salar L*). Aquaculture 545, 737203. https://doi.org/10.1016/j.aquaculture.2021.737203.
Pacorig, V., Galeotti, M., Beraldo, P., 2022. Multiparametric semi-quantitative scoring system for the histological evaluation of marine fish larval and juvenile quality. Aquac. Rep. 26, 101285. https://doi.org/10.1016/j.aqrep.2022.101285.
Pan, H.-H., Setiawan, A.N., McQueen, D., Khan, J.R., Herbert, N.A., 2020. Elevated CO2 concentrations impacts growth and swimming metabolism in yellowtail kingfish, *Seriola lalandi*. Aquaculture 523, 735157. https://doi.org/10.1016/j.aquaculture.2020.735157.
Pedregosa, F., Thirion, B., Varoquaux, G., Org, N., Gramfort, A., Michel, V., Fr, L., Thirion, B., Grisel, O., Blondel, M., Prettenhofer, P., Weiss, R., Dubourg, V., Vanderplas, J., Passos, A., Tp, A., Cournapeau, D., 2011. Scikit-learn: machine learning in Python. J. Mach. Learn. Res. 12, 2825–2830.
Pierce, R.H., Weeks, J.M., Prappas, J.M., 1993. Nitrate toxicity to five species of marine fish. J. World Aquacult. Soc. 24, 105–107. https://doi.org/10.1111/j.1749-7345.1993.tb00156.x.
Polistovskaya, P.A., Karpenko, L.Y., Bakhta, A.A., Kinarevskaya, K.P., Enukashvili, A.I., 2018. Desquamation of Intestinal Epithelium as Indicator of Toxicosis in Fish. Presented at the International Scientific and Practical Conference "Agro-SMART - SMART Solutions for Agriculture" (Agro-SMART 2018),. Atlantis Press, pp. 569–573. https://doi.org/10.2991/agrosmart-18.2018.106.
Poortenaar, C.W., Hooker, S.H., Sharp, N., 2001. Assessment of yellowtail kingfish (*Seriola lalandi lalandi*) reproductive physiology, as a basis for aquaculture development. Aquaculture 201, 271–286. https://doi.org/10.1016/S0044-8486(01)00549-X.
Preena, P.G., Rejish Kumar, V.J., Singh, I.S.B., 2021. Nitrification and denitrification in recirculating aquaculture systems: the processes and players. Rev. Aquac. 13, 2053–2075. https://doi.org/10.1111/raq.12558.
Price, M.N., Dehal, P.S., Arkin, A.P., 2010. FastTree 2 – approximately maximum-likelihood trees for large alignments. PLoS One 5, e9490. https://doi.org/10.1371/journal.pone.0009490.
Quast, C., Pruesse, E., Yilmaz, P., Gerken, J., Schweer, T., Yarza, P., Peplies, J., Glöckner, F.O., 2013. The SILVA ribosomal RNA gene database project: improved data processing and web-based tools. Nucleic Acids Res. 41, D590–D596. https://doi.org/10.1093/nar/gks1219.
R Core Team, 2024. R: A Language and Environment for Statistical Computing.
Ramírez, C., Romero, J., 2017. The microbiome of Seriola lalandi of wild and aquaculture origin reveals differences in composition and potential function. Front. Microbiol. 8. https://doi.org/10.3389/fmicb.2017.01844.
Rangaswamy, B., Ramankutty Nair, R., Achuthan, C., Isaac Sarojini, B.S., 2020. Computational analysis of successional changes in the microbial population and community diversity of the immobilized marine nitrifying bacterial consortium in a nitrifying packed bed bioreactor. 3 Biotech 10, 524. https://doi.org/10.1007/s13205-020-02510-z.
Romalde, J.L., 2002. Photobacterium damselae subsp. piscicida: an integrated view of a bacterial fish pathogen. Int. Microbiol. 5, 3–9. https://doi.org/10.1007/s10123-002-0051-6.
Ruan, Y., Guo, X., Ye, Z., Liu, Y., Zhu, S., 2015. Bacterial community analysis of different sections of a biofilter in a full-scale marine recirculating aquaculture system. N. Am. J. Aquac. 77, 318–326. https://doi.org/10.1080/15222055.2015.1017128.
Rurangwa, E., Verdegem, M.C.J., 2015. Microorganisms in recirculating aquaculture systems and their management. Rev. Aquac. 7, 117–130. https://doi.org/10.1111/raq.12057.
Russo, R.C., Thurston, R.V., 1991. Toxicity of Ammonia, Nitrite, and Nitrate to Fishes. Book chapter (No. PB-92-179142/XAB; EPA-600/A-92/089). Environmental Protection Agency, Athens, GA (United States). Environmental Research Lab.
Ruyet, J.P.-L., Chartois, H., Quemener, L., 1995. Comparative acute ammonia toxicity in marine fish and plasma ammonia response. Aquaculture 136, 181–194. https://doi.org/10.1016/0044-8486(95)01026-2.
Saraiva, A., Costa, J., Serrão, J., Cruz, C., Eiras, J.C., 2015. A histology-based fish health assessment of farmed seabass (*Dicentrarchus labrax* L.). Aquaculture 448, 375–381. https://doi.org/10.1016/j.aquaculture.2015.06.028.
Saraiva, A., Costa, J., Eiras, J.C., Cruz, C., 2016. Histological study as indicator of juveniles farmed turbot, *Scophthalmus maximus* L. health status. Aquaculture 459, 210–215. https://doi.org/10.1016/j.aquaculture.2016.03.048.
Schneider, C.A., Rasband, W.S., Eliceiri, K.W., 2012. NIH image to ImageJ: 25 years of image analysis. Nat. Methods 9, 671–675. https://doi.org/10.1038/nmeth.2089.
Schram, E., Roques, J.A.C., Abbink, W., Yokohama, Y., Spanings, T., de Vries, P., Bierman, S., van de Vis, H., Flik, G., 2014. The impact of elevated water nitrate concentration on physiology, growth and feed intake of African catfish larias gariepinus (Burchell 1822). Aquac. Res. 45, 1499–1511. https://doi.org/10.1111/are.12098.
Schreier, H.J., Mirzoyan, N., Saito, K., 2010. Microbial diversity of biological filters in recirculating aquaculture systems. Curr. Opin. Biotechnol. 21, 318–325. https://doi.org/10.1016/j.copbio.2010.03.011.
Sellyei, B., Varga, Z., Cech, G., Varga, Á., Székely, C., 2021. Mycoplasma infections in freshwater carnivorous fishes in Hungary. J. Fish Dis. 44, 297–304. https://doi.org/10.1111/jfd.13283.
Siikavuopio, S.I., Sæther, B.-S., 2006. Effects of chronic nitrite exposure on growth in juvenile Atlantic cod, *Gadus morhua*. Aquaculture 255, 351–356. https://doi.org/10.1016/j.aquaculture.2005.11.058.
Sitjà-Bobadilla, A., Estensoro, I., Pérez-Sánchez, J., 2016. Immunity to gastrointestinal microparasites of fish. Dev. Comp. Immunol. 64, 187–201. https://doi.org/10.1016/j.dci.2016.01.014. Special Issue: Intestinal Immunity.
Smith, L.L., Oseid, D.M., 1974. Effect of hydrogen sulfide on development and survival of eight freshwater fish species. In: The Early Life History of Fish. Springer, Berlin Heidelberg, pp. 417–430. https://doi.org/10.1007/978-3-642-65852-5_34.
Sommerset, I., Walde, S.C., Bang Jensen, B., Bornø, G., Haukaas, A., Brun, E.(red)., 2020. The Health Situation in Norwegian Aquaculture 2019 - Norwegian Veterinary Institute Report Series nr 5b/2020, pp. 1–156.
Stadtländer, C., Kirchhoff, H., 1990. Surface parasitism of the fish mycoplasma *Mycoplasma mobile* 163 K on tracheal epithelial cells. Vet. Microbiol. 21, 339–343. https://doi.org/10.1016/0378-1135(90)90005-G.
Strzyzewska, E., Szarek, J., Babinska, I., 2016. Morphologic evaluation of the gills as a tool in the diagnostics of pathological conditions in fish and pollution in the aquatic environment: a review. Vet. Med. (Praha) 61, 123–132. https://doi.org/10.17221/8763-VETMED.
Summerfelt, S.T., Vinci, B.J., Piedrahita, R.H., 2000. Oxygenation and carbon dioxide control in water reuse systems. Aquac. Eng. 22, 87–108. https://doi.org/10.1016/S0144-8609(00)00034-0.
Symonds, J., Walker, S.P., Pether, S., Gublin, Y., McQueen, D., King, A., Irvine, G.W., Setiawan, A.N., Forsythe, J.A., Bruce, M., 2014. Developing yellowtail kingfish (*Seriola lalandi*) and hāpuku (*Polyprion oxygeneios*) for New Zealand aquaculture. N. Z. J. Mar. Freshw. Res. 48, 371–384. https://doi.org/10.1080/00288330.2014.930050.
Takahashi, A., Shiroishi, T., Koide, T., 2014. Genetic mapping of escalated aggression in wild-derived mouse strain MSM/Ms: association with serotonin-related genes. Front. Neurosci. 8. https://doi.org/10.3389/fnins.2014.00156.
Timmons, M., Guerdat, T., Vinci, B., 2018. Recirculating Aquaculture, 4th edition. Ithaca Publishing Company, Ithaca.
Tomasso, J.R., 1994. Toxicity of nitrogenous wastes to aquaculture animals. Rev. Fish. Sci. 2, 291–314. https://doi.org/10.1080/10641269409388560.
Toranzo, A.E., 2004. Report about fish bacterial diseases. Mediterr. Aquac. Diagn. Lab. 49–89.
Toranzo, A., Magariños, B., Romalde, J., 2005. A review of the main bacterial fish diseases in mariculture systems. Aquaculture 246, 37–61. https://doi.org/10.1016/j.aquaculture.2005.01.002.
Untergrasser, A., Cutcutache, I., Koressaar, T., Ye, J., Faircloth, B., Remm, M., Rozen, S., 2012. Primer3–new capabilities and interfaces. Nucleic Acids Res. 40 (15), e115. https://doi.org/10.1093/nar/gks596.
Urakawa, H., Tajima, Y., Numata, Y., Tsuneda, S., 2008. Low temperature decreases the phylogenetic diversity of ammonia-oxidizing archaea and bacteria in aquarium biofiltration systems. Appl. Environ. Microbiol. 74, 894–900. https://doi.org/10.1128/AEM.01529-07.
Vadstein, O., Bergh, Ø., Gatesoupe, F.-J., Galindo-Villegas, J., Mulero, V., Picchietti, S., Scapigliati, G., Makridis, P., Olsen, Y., Dierckens, K., Defoirdt, T., Boon, N., De Schryver, P., Bossier, P., 2013. Microbiology and immunology of fish larvae. Rev. Aquac. 5, S1–S25. https://doi.org/10.1111/j.1753-5131.2012.01082.x.

Vadstein, O., Attramadal, K.J.K., Bakke, I., Olsen, Y., 2018. K-selection as microbial community management strategy: A method for improved viability of larvae in aquaculture. Front. Microbiol. 9. https://doi.org/10.3389/fmicb.2018.02730.

van Bussel, C.G.J., Schroeder, J.P., Wuertz, S., Schulz, C., 2012. The chronic effect of nitrate on production performance and health status of juvenile turbot (*Psetta maxima*). Aquaculture 326–329, 163–167. https://doi.org/10.1016/j.aquaculture.2011.11.019.

Wajsbrot, N., Gasith, A., Diamant, A., Popper, D.M., 1993. Chronic toxicity of ammonia to juvenile gilthead seabream Sparus aurata and related histopathological effects. J. Fish Biol. 42, 321–328. https://doi.org/10.1111/j.1095-8649.1993.tb00336.x.

Weber, B., Chen, C., Milton, D.L., 2010. Colonization of fish skin is vital for Vibrio anguillarum to cause disease. Environ. Microbiol. Rep. 2, 133–139. https://doi.org/10.1111/j.1758-2229.2009.00120.x.

Wolf, J.C., 2018. Comparing apples and oranges and pears and kumquats: the misuse of index systems for processing histopathology data in fish toxicological bioassays. Environ. Toxicol. Chem. 37, 1688–1695. https://doi.org/10.1002/etc.4117.

Wolf, J.C., Baumgartner, W.A., Blazer, V.S., Camus, A.C., Engelhardt, J.A., Fournie, J.W., Frasca, S., Groman, D.B., Kent, M.L., Khoo, L.H., Law, J.M., Lombardini, E.D., Ruehl-Fehlert, C., Segner, H.E., Smith, S.A., Spitsbergen, J.M., Weber, K., Wolfe, M.J., 2015. Nonlesions, misdiagnoses, missed diagnoses, and other interpretive challenges in fish histopathology studies:a guide for investigators, authors, reviewers, and readers. Toxicol. Pathol. 43, 297–325. https://doi.org/10.1177/0192623314540229.

Yoon, J., Lee, E.-Y., Nam, S.-J., 2022. Erythrobacter rubeus sp. nov., a carotenoid-producing alphaproteobacterium isolated from coastal seawater. Arch. Microbiol. 204, 125. https://doi.org/10.1007/s00203-021-02736-2.

Zawisza, M., Chadzinska, M., Steinhagen, D., Rakus, K., Adamek, M., 2024. Gill disorders in fish: lessons from poxvirus infections. Rev. Aquac. 16, 234–253.

Zhang, X.-H., He, X., Austin, B., 2020. Vibrio harveyi: a serious pathogen of fish and invertebrates in mariculture. Mar. Life Sci. Technol. 2, 231–245. https://doi.org/10.1007/s42995-020-00037-z.